Phosphorylation of mitochondrial matrix proteins regulates their selective mitophagic degradation

Panagiota Kolitsida[1], Jianwen Zhou[2], Michal Rackiewicz[2], Jörn Dengjel[2,3] and Hagai Abeliovich[1]

Address correspondence to: Dr. Hagai Abeliovich, Dept. of Biochemistry and Food Science, Hebrew University of Jerusalem, Rehovot, Israel 76100, Tel: 972-8-9489060; Fax: 972-8-9476189; E-mail: hagai.abeliovich@mail.huji.ac.il

1 Dept. of Biochemistry, Food Science and Nutrition, Hebrew University of Jerusalem, Rehovot, Israel

2 Department of Biology, University of Fribourg, Chemin du Musée 10, 1700 Fribourg, Switzerland

3 Department of Dermatology, Medical Center - University of Freiburg, Hauptstr. 7, 79104 Freiburg, Germany

Abstract

Mitophagy is an important quality control mechanism in eukaryotic cells, and defects in mitophagy correlate with aging phenomena and neurodegenerative disorders. It is known that different mitochondrial matrix proteins undergo mitophagy with very different rates, but to date the mechanism underlying this selectivity at the individual protein level has remained obscure. We now present evidence indicating that protein phosphorylation within the mitochondrial matrix plays a mechanistic role in regulating selective mitophagic degradation in yeast, via involvement of the Aup1 mitochondrial protein phosphatase, as well as two known matrix-localized protein kinases, Pkp1 and Pkp2. By focusing on a specific matrix phosphoprotein reporter, we also demonstrate that phospho-mimetic and non-phosphorylatable point mutations at known phosphosites in the reporter increased or decreased its tendency to undergo mitophagy. Finally, we show that phosphorylation of the reporter protein is dynamically regulated during mitophagy, in an Aup1-dependent manner. Our results indicate that structural determinants on a mitochondrial matrix protein can govern its mitophagic fate, and that protein phosphorylation regulates these determinants and segregates proteins into sub-compartments destined for mitophagic degradation.

Keywords:
mitophagy/autophagy/mitochondria/phosphorylation/phosphatase/Saccharomyces cerevisiae

Introduction

Mitochondrial autophagy, or mitophagy, is considered an important quality control mechanism in eukaryotic cells (Green *et al*., 2011; Bratic and Larsson, 2013; Dengjel and Abeliovich, 2016). Defects in mitophagic clearance of malfunctioning mitochondria have been proposed to play a role in the pathogenesis of neurological disorders such as Parkinson's, Alzheimer's and Huntington's diseases (Narendra and Youle, 2011; Corsetti *et al*., 2015; Pickrell and Youle, 2015; Banerjee *et al*., 2016; Guo *et al*., 2016) and may be associated with additional aging-related pathologies (Diot *et al*., 2016). As with other forms of selective autophagy, mitophagy is induced by the activation of a receptor protein, or by its recruitment to the organellar surface. The receptor interacts with the autophagic machinery to mediate the engulfment of specific mitochondria which are designated for degradation (Kanki *et al*., 2015; Abeliovich and Dengjel, 2016). In many mammalian cell types, loss of mitochondrial membrane potential stabilizes the PINK1 protein kinase on the outer mitochondrial membrane (Narendra *et al*., 2010). This leads to the PINK1-dependent recruitment and phosphorylation of Parkin, a ubiquitin E3 ligase (Narendra *et al*., 2008; Kondapalli *et al*., 2012; Shiba-Fukushima *et al*., 2012), as well as to the local production of phospho-ubiquitin (Kane *et al*., 2014; Kazlauskaite *et al*., 2014; Koyano *et al*., 2014; Ordureau *et al*., 2014). Phospho-ubiquitylation of mitochondrial outer membrane proteins recruits the soluble mitophagy receptors NDP52 and optineurin, which link the defective mitochondrial compartment with the autophagic machinery and mediate its degradation (Lazarou *et al*., 2015). Mitophagy has also been implicated in specific developmental transitions in mammals, such as muscle, neuron, and erythrocyte differentiation (Sandoval *et al*., 2008; Mortensen *et al*., 2010; Novak *et al*., 2010; Sin *et al*., 2016; Esteban-Martínez *et al*., 2017). In yeast cells, the Atg32 mitophagy receptor is a type 2 mitochondrial outer membrane protein which is found on all mitochondria (Kanki *et al*., 2009; Okamoto *et al*., 2009), but undergoes post-translational modifications which activate it, presumably on specific mitochondria which are thus marked for degradation (Aoki *et al*., 2011; Farré *et al*., 2013; Wang *et al*., 2013).

An important question is whether the representation of matrix proteins in mitochondria destined for degradation is identical to the average representation in the general mitochondrial network. We previously determined that in *Saccharomyces cerevisiae*, different mitochondrial matrix protein reporters undergo mitophagy at drastically different rates, indicating the existence of a pre-engulfment sorting mechanism (Abeliovich *et al*., 2013). We were also able to show that altering mitochondrial dynamics, through deletion of the *DNM1* gene, affected the selectivity that is observed, even though mitochondrial dynamics is not absolutely essential for mitophagy per se, as also confirmed by others

(Yamashita *et al*., 2016). These results led us to speculate that mitochondrial dynamics, through repeated mitochondrial fission and fusion cycles, is able to distill defective components from the network, while sparing other molecular species (Abeliovich *et al*., 2013; Dengjel and Abeliovich, 2014). However, while fission and fusion can 'shake up' the network by mixing components, a distillation process would also require some kind of physical segregation principle. A hint into the nature of the putative segregation principle could be related to the function of the mitochondrial phosphatase Aup1 (also known as Ptc6). Aup1 was originally identified by virtue of a synthetic genetic interaction with the Atg1 protein kinase (Tal *et al*., 2007). Loss of this gene leads to defects in mitophagy when assayed by some methods, but not by other methods (Tal *et al*., 2007; González *et al*., 2013). The finding that mitophagy could be protein-specific at the intra-mitochondrial level suggests the possibility that Aup1 could be involved in generating and maintaining mitophagic selectivity, as this would explain the different experimental outcomes obtained using different reporters and conditions. In the present work, we demonstrate that perturbations of mitochondrial protein phosphorylation caused by mutating *AUP1* and additional genes encoding mitochondrial kinases, affect the selectivity of mitophagy. We also show that point mutations at specific phosphosites in a known mitochondrial matrix phosphoprotein, Mdh1, affect the mitophagic efficiency of the protein, and that mitophagic efficiency of Mdh1-GFP is determined downstream of Aup1 function. Thus, our data indicate that targeting of individual protein molecules for mitophagy depends on specific structural determinants and can be further regulated by protein phosphorylation.

Results

A role for mitochondrial phosphatases and kinases in regulating the intra-mitochondrial selectivity of stationary phase mitophagy

Aup1, a conserved PP2C- type mitochondrial phosphatase, was previously shown to be required for efficient stationary phase mitophagy, using a simplistic assay which follows the levels of Aco1 (one of two mitochondrial aconitase isoforms in yeast) over the time course of stationary phase mitophagy (Tal *et al*., 2007). To test the involvement of Aup1 in mitophagy using more up-to-date methods, we followed the effects of deleting *AUP1* in yeast expressing a chimeric Mdh1-GFP fusion protein. As previously shown for other reporter proteins, delivery of the GFP chimera to the vacuole results in degradation of the native Mdh1 moiety while the residual GFP portion is resistant to vacuolar proteases, generating the appearance of free GFP in immunoblots (Klionsky *et al*., 2012). This can then be used as a semi-quantitative readout of the efficiency of mitophagy (Figure 1). We find that Aup1 is required for mitophagic degradation of Mdh1-GFP, and that this phenotype is complemented by expression of the *AUP1* gene from a plasmid (Figure 1A). Complementation depends on the 34 amino terminal amino acid residues of the protein, which are predicted to contain the mitochondrial targeting sequence. Deletion of the *ATG32* gene completely abrogates the appearance of free GFP (Figure 1B), validating that the free GFP appears specifically as a result of mitophagic trafficking, and not due to another autophagic pathway or other degradation mechanisms (this control was repeated for all mitochondrial GFP fusion proteins used in this study, with identical results; see supplementary Figure 1).

The defect in mitophagic trafficking of Mdh1 in *aup1Δ* cells (Figure 2B) can be overcome by overexpressing Mdh1-GFP from a plasmid (Figure 2A), suggesting the existence of a saturable selectivity mechanism. This saturation is not a specific property of Mdh1, as the same observation was made when using an Idp1-GFP fusion protein as a reporter (Figure 2C-D). In addition, we tested the effects of deleting Aup1 on the mitophagic trafficking of Aco1, Aco2, and Qcr2, which are also localized to the mitochondrial matrix. We find that while Aco1, Mdh1 and Idp1 are affected by knocking out the *AUP1* gene, Aco2 and Qcr2 are less significantly impacted by this mutation (Figure 3). Interestingly, Aco1 and Aco2 are 55% identical in sequence, but Aco1 is a known phosphoprotein while Aco2 has not been reported to be phosphorylated. Yeast mitochondria are known to contain at least two kinases (Pkp1 and Pkp2) and at least two phosphatases (Ptc5 and Aup1). To determine whether the role of Aup1 reflects a broader involvement of protein phosphorylation in determining selectivity, we tested the same 5 reporter proteins for their ability to undergo mitophagy in wild-type,

aup1Δ, *ptc5Δ*, *pkp1Δ*, and *pkp2Δ* cells (Figure 3A). As previously shown, WT cells exhibit different efficiencies of generation of free GFP for different mitochondrial reporters, under mitophagy-inducing conditions. We then compared the mitophagic selectivity of the different genotypes by calculating pairwise Pearson correlation coefficients, followed by a clustering analysis of the respective data vectors representing each genotype (Figure 3B-C). We find that, while Ptc5 does not play an appreciable role in regulating mitophagic selectivity (at least with respect to the reporters assayed here), the deletion of either *PKP1* or *PKP2* led to selectivity profiles that were similar to those observed for the deletion of *AUP1* (Figure 3B and supplementary Figure 2). This result is consistent with mitochondrial protein phosphorylation playing a general role in determining the intra-mitochondrial selectivity of mitophagic trafficking, not restricted to Aup1 function alone. In fact, the double deletion mutant *pkp1Δ pkp2Δ* effectively shuts down mitophagy for most of the reporters we have tested here (Figure 3A), except for Aco1-GFP, which is inhibited by about 40% in this genetic background.

Mdh1, a mitochondrial matrix protein, is phosphorylated on serine 196, threonine 199 and serine 240 during growth on lactate under mitophagy-inducing conditions

Many mitochondrial matrix proteins are known to undergo phosphorylation (Reinders *et al*., 2007), although the precise physiological role of these modifications is generally unclear. The apparent involvement of mitochondrial kinases and phosphatases in regulating mitophagic specificity suggests that, at least in some cases, protein phosphorylation can affect mitophagic fate. We therefore tested whether Mdh1-GFP, a reporter which shows a high sensitivity to deletion of Aup1, is indeed phosphorylated under our working conditions. Mdh1, encoding malate dehydrogenase, contains 5 known phosphosites, at positions 59, 177, 196, 199, and 240 (Reinders *et al*., 2007; Holt *et al*., 2009; Swaney *et al*., 2013). As shown in Figure 4, we found by LC-MS/MS analysis of denatured protein extracts that S196, T199 and S240 in Mdh1 are phosphorylated under our working conditions.

Structural determinants on Mdh1 regulate mitophagic efficiency 'in cis'

If matrix protein phosphorylation plays a role in determining mitophagic selectivity, then we should expect that site-directed mutagenesis of phosphosites on such a protein would affect its rate of mitophagy. We carried out site-directed mutagenesis of the sites identified by us (Figure 4), as well as of other reported Mdh1 phosphosites, to the respective alanine and aspartate variants. When the corresponding GFP fusion chimeras were expressed in yeast cells, we could observe that the T59A, S196A and T199A mutants were unable to undergo mitophagy, while the S240A variant reproducibly

showed increased mitophagic efficiency relative to wild-type (Figure 5A). The inability of the T59A, S196A and T199A mutants to undergo mitophagy does not reflect a general block of mitophagy in these cells: a co-expressed mtRFP showed clear induction of mitophagy, as judged by the appearance of red fluorescence in the vacuole, while the T59A and T199A variants maintained a mostly mitochondrial localization (Figure 5B). This result also makes it unlikely that the point mutants are delivered to the vacuole, but for some reason are recalcitrant to degradation by vacuolar proteases. To further rule out the possibility that differences in sensitivity to vacuolar proteases underlie the difference in release of free GFP from Mdh1-GFP between WT and the T199A mutant, we deleted the mitochondrial targeting sequence in these constructs. The resultant Mdh1-GFP molecules are cytoplasmic, and can be directly targeted to the vacuole by nitrogen-starvation induced macroautophagy, thus completely bypassing mitochondria (Torggler *et al*., 2017). If the difference observed between WT Mdh1-GFP and the T199A mutant is due to differential sensitivity to vacuolar proteases, then we expect it to persist in constructs lacking the MTS under general macroautophagy-inducing conditions, as the path taken en route to the vacuole should not affect the sensitivity to proteolysis within the vacuole. However, in the experiment shown in Figure 5C, we can see that both MTSΔ constructs generate very similar amounts of free GFP upon nitrogen starvation, in stark contrast with the respective mitochondrially-targeted constructs. In addition, the free GFP which is formed from the MTSΔ constructs is indeed due to direct macroautophagic transport from the cytosol to the vacuole, as it is independent of Atg32, but totally dependent on Atg1. Thus, we can conclude that discrete changes to a protein's structure can have a clear effect on its mitophagic targeting without affecting mitophagic targeting of other mitochondrial proteins.

If the effects of the threonine to alanine and serine to alanine mutations reflect effects due to phosphorylation, one would expect that at least in some of the cases, the corresponding aspartate mutations should have a reciprocal effect. Indeed some of the corresponding aspartate variants of Mdh1-GFP showed such a reciprocal effect, relative to the alanine mutants. Thus, mitophagic targeting of the S240D mutant is strongly attenuated relative to the wild type, and the mitophagic targeting of the T199D mutant is increased, relative to wild-type (see Figure 5D).

Time and Aup1-dependent changes in the phosphorylation state of Mdh1-GFP occur during mitophagy

To gain a better understanding of the role of phosphorylation in directing mitophagic selectivity, we analyzed time- and genotype- dependent changes in the phosphorylation state of Mdh1-

GFP during mitophagy. Native immunoprecipitation of Mdh1-GFP from protease-deficient (*pep4Δ* genetic background) followed by immunoblotting with anti phosphoserine/phosphothreonine antibody (anti pSer/pThr) identifies a λ-phosphatase sensitive signal which increases in WT cells over the incubation period, but decreases over time in the isogenic *aup1Δ* strain, and is undetectable by day 2-3 of the incubation, when mitophagy is normally induced (Figure 6A, 6B).

We also managed to quantify peptides containing phosphor-Ser196 and phosphor-Thr199 by SILAC-based mass spectrometry, comparing WT to *aup1Δ* cells. At day 2, phosphoSer196 appears to be stable, whereas phosphoThr199 is significantly less abundant in *aup1Δ* cells relative to *AUP1* expressing cells (Figure 6C). Thus, we conclude that the reduced phosphorylation of Thr199 contributes to the decrease of phosphoSer/Thr signal observed by western blot analysis of anti-GFP immunoprecipitates in *aup1Δ* cells (Figure 6A).

Expression of a hyper-mitophagy variant of Mdh1-GFP can suppress mitophagy defects in *aup1Δ* and *pkp2Δ* cells.

If phosphorylation of Mdh1 at T199 is important for mitophagic trafficking of the protein, and if Aup1 directly or indirectly regulates the phosphorylation state at this residue, then we expect the T199D mutant to be able, at least partially, to bypass the phenotype of the *aup1Δ* or *pkp2Δ* mutations. Similarly, we might expect effects for the S240A mutant, which also shows increased mitophagic trafficking relative to WT. As shown in Figure 7A and 7B, the T199D mutation shows reproducible suppression of both the *aup1Δ* and *pkp2Δ* mutants. However, neither of the position 240 mutants was able to bypass the *aup1Δ* mutation. These results clearly indicate that modification of Mdh1 at position 199 can regulate mitophagic trafficking of Mdh1-GFP downstream of Aup1 and Pkp2. Double mutation analysis using the two positions suggests bimodal, independent regulation at the two sites: If phosphorylation at 240 was simply regulating phosphorylation at 199, we would expect the double aspartate mutation to suppress the *aup1Δ* phenotype, but this is not the case (Figure 7; see discussion).

Overexpression of Pkp2, but not Pkp1, can bypass the mitophagic defect of Mdh1-GFP in *aup1Δ* cells

Deletion of *AUP1* leads to hypo-phosphorylation of Mdh1-GFP, as judged by anti-phosphoamino acid immunoblot (Figure 6). This makes it very unlikely that the effects of Aup1 are due to direct dephosphorylation of Mdh1 by the phosphatase. Alternatively, *AUP1* could regulate Pkp1 and/or Pkp2 which will, in turn, regulate the phosphorylation state of Mdh1. To test this second possibility, we overexpressed either Pkp1 or Pkp2 in *aup1Δ* cells, and assayed delivery of Mdh1-GFP to the vacuole under mitophagy inducing conditions through release of free GFP. As shown in Figure 7C, the overexpression of Pkp2, but not Pkp1, allowed free GFP release from Mdh1-GFP in *aup1Δ* cells. This result is consistent with Pkp2 functioning downstream of Aup1, in regulating Mdh1-GFP mitophagic clearance. In further support of this interpretation, overexpression of Pkp2 rescues the hypophosphorylation of Mdh1-GFP in *aup1Δ* cells (Figure 7D): While *aup1Δ* cells harboring empty vector show hypophosphorylation of Mdh1-GFP, *aup1Δ* cells overexpressing Pkp2 show a clear recovery of the anti-phosphoamino acid immunoblot signal. This result strongly indicates that Aup1 regulates Pkp2 activity, which in turn regulates the phosphorylation state of Mdh1-GFP.

Deletion of *AUP1* leads to changes in the protein interaction network of Mdh1-GFP

To probe the mechanism by which changes in phosphorylation pattern affect mitophagic efficiency of Mdh1-GFP, we assayed protein-protein interactions of Mdh1 by immunoprecipitation from WT and *aup1Δ* cells at different time points during the timeline of our mitophagy induction protocol. We tested the co- immunoprecipitation of Mdh1-GFP with Mic60-HA and with Cit1-HA, both of which were previously reported to interact with Mdh1 (Vélot *et al*., 1999; von der Malsburg *et al*., 2011). As shown in Figure 8, we were able to recapitulate both interactions under our experimental conditions. Strikingly however, The Mic60 interaction was stronger in the *aup1Δ* mutant relative to WT on day 1, and these interactions, in both mutant and WT, weakened considerably between days 1 and 4 of the incubation (Figure 8A) such that the interaction in WT cells became undetectable in the day 4 sample. The Cit1-Mdh1 interaction was far stronger in the *aup1Δ* mutant than in WT (where the interaction was below our detection limit) and increased at day 4 in the mutant, relative to day 1 (Figure 8B). Thus, deletion of *AUP1* has drastic and divergent effects on the Mdh1 interactome, which may underlie its effects on mitophagic targeting of the protein.

Deletion of *AUP1*, and point mutations which abrogate mitophagic trafficking of Mdh1, alter the distribution of the Mdh1-GFP reporter protein within the mitochondrial network

We previously published that GFP chimeras of protein species which display less mitophagic efficiency appear to be segregated within the network, relative to a generic mitochondrial RFP reporter (Abeliovich *et al.*, 2013). We therefore wanted to analyze whether the various molecular perturbations which were found to affect mitophagic trafficking in the present study, will also affect the distribution of the Mdh1-GFP reporter protein within the mitochondrial network. As shown in Figure 9A, there is a clear difference in the distribution of Mdh1-GFP between WT cells and *aup1Δ* cells at day 2 of the incubation, with *aup1Δ* cells exhibiting apparent clumping of the GFP signal to discrete dots within the mitochondrial network as defined by the mtRFP signal. Consistent with this finding, Figure 9B illustrates that wild-type Mdh1-GFP, and a point mutant which does not reduce mitophagic trafficking, (S240A), show a statistically significant increase in the signal overlap of the red and the green channels between day 1 and day 2 of the incubation, as determined using the JACoP plugin (Bolte and Cordelières, 2006). In contrast, we observed that mutants which do show a significant block in mitophagic trafficking display a statistically significant decrease in signal overlap (relative to mtRFP) from day 1 to day 2, similar to that observed in the *aup1Δ* strains. It is important to note that none of the mutations tested had any effect on the general fractionation properties of Mdh1-GFP (see supplementary figure 8) making it unlikely that they affect targeting of the protein into mitochondria. Rather, the data is consistent with some degree of segregation of these mutants, relative to the overall available space in the mitochondrial matrix as defined by the mtRFP fluorescence signal. Thus, inability of the reporter to undergo mitophagy correlates with a segregation phenomenon within the mitochondrial matrix.

Discussion

In this study, we find that protein phosphorylation in the mitochondrial matrix plays a role in contributing to the selectivity of mitophagic degradation. We show that the selectivity filter depends on specific structural determinants in an individual mitochondrial matrix protein, and that the phosphorylation state of the protein can regulate the function of these determinants. The finding that within an individual protein species, differentially modified forms of the protein can have different mitophagic fates constitutes an important advance in our mechanistic understanding of the selectivity phenomenon. It suggests that specific 'degron-like elements' on mitochondrial matrix proteins are regulating selectivity and this now allows further analysis of the molecular mechanism. While individual mitochondrial phosphatases and kinases each affect a subset of mitochondrial proteins, sometimes incompletely, we found that knockout of both mitochondrial kinases (Pkp1 and Pkp2) completely blocked mitophagic trafficking of nearly all the reporters tested in this study. Therefore, we can conclude that matrix protein phosphorylation is a widespread determinant of mitophagic selectivity.

We further demonstrate that a novel protein phosphorylation cascade plays a role in the regulation of selectivity. The Aup1 phosphatase functions upstream of the Pkp2 kinase in this cascade, as 1) the Mdh1^{T199D} mutant was able to partially bypass the specific requirements for Aup1 and Pkp2 (Figures 5D and 7B). 2) it is unlikely that direct dephosphorylation of threonine 199 by Aup1 is responsible, since the phosphomimic mutations point to the phosphorylated form of T199 as being 'mitophagy competent' (Figures 5A, 5D, 7A, and 7B). It is much more likely that Aup1 is required, directly or indirectly, for the activation of a kinase such as Pkp2. Indeed, we found that overexpression of Pkp2, but not Pkp1, can suppress both the Mdh1 mitophagy defect (Figure 7C) and the hypophosphorylation of Mdh2 (Fig. 7D) which are observed in *aup1Δ* cells. This strongly suggests that Aup1 activity is required for activation of Pkp2, and that Pkp2 directly phosphorylates Mdh1 at position 199. The fact that the S240D mutation is able to prevent rescue of the *aup1Δ* phenotype by T199D in the context of the S240D T199D double mutant (Figure 7A), may suggest that the two sites represent a combinatorial output, not a strictly hierarchical one where position 240 affects the phosphorylation state of threonine 199.

The two known yeast mitochondrial kinases (Pkp1 and Pkp2) have been identified as orthologs of mammalian PDKs (pyruvate dehydrogenase kinases), which exist as a family of paralogs with

different tissue distribution in metazoans (Steensma *et al.*, 2008). Reports in the literature (Krause-Buchholz *et al.*, 2006; Gey *et al.*, 2008) also link the two phosphatases, Ptc5 and Aup1 (Ptc6) to Pda1 dephosphorylation in yeast. We were unable to test for a direct role of Pda1 in mitophagy, as the deletion mutant shows severely impaired growth in our liquid SL medium. Nonetheless, our data are not consistent with Pda1 phosphorylation being the determinant of mitophagic selectivity and efficiency in our experiments, for the following reasons. First of all, yeast Pda1 has only one verified phosphosite which is regulated by these enzymes: serine 313. Thus, if all of these mitochondrial kinases and phosphatases in yeast converge exclusively on the regulation of Pda1, then we expect Aup1 and Ptc5 to have opposite phenotypes relative to Pkp1 and Pkp2. However, our results are inconsistent with this prediction, and indicate that Aup1 functions to regulate and activate Pkp2 in our readouts. In addition, the apparent lack of involvement of Ptc5 and the non-redundant role of Aup1 in the phenotypes observed also argue against an interpretation which converges on Pda1 phosphorylation. Finally, one should note that there are hundreds of documented phosphorylation sites in yeast mitochondrial proteins (Reinders *et al.*, 2007; Renvoisé *et al.*, 2014) and it is therefore unlikely that the only role of Aup1, Ptc5, Pkp1 and Pkp2 is to regulate phosphorylation of serine 313 on Pda1.

Yeast cells are not the only system in which protein-level specificity was observed during mitophagy. Hämäläinen *et al* (Hämäläinen *et al*., 2013) showed that in differentiation of MELAS patient-derived iPSCs into neurons, mitochondrial respiratory chain (RC) complex I (CI) underwent a selective mitophagic degradation process which spared other RC components. In addition, they could show that the remaining CI in these cells was segregated into distinct patches within the mitochondrial network, while other RC components were evenly distributed. Their results demonstrate that intra-mitochondrial selectivity of mitophagic degradation also occurs in mammalian cells, and is not restricted to yeast. Interestingly, phosphorylation of complex I components has been reported in mammalian cells (Papa *et al*., 2010). In cultured mammalian cells, Burman et al demonstrated selective mitophagic clearance of a mutant ornithine transcarbamoylase (Burman *et al*., 2017).

How can we envision the effects of posttranslational matrix protein modification on mitophagic selectivity of individual protein molecules? We previously proposed that phase separation within the mitochondrial matrix, coupled with repeated fission and fusion cycles, would lead to a distillation effect where the "minority" phase would be segregated and restricted to homogeneous mitochondrial compartments (Abeliovich *et al*., 2013; Dengjel and Abeliovich, 2014). If phosphorylation, or any other modification, affects the partitioning of a given protein molecule between these phases, then it would also affect the protein's segregation tendencies. We then need to postulate that the accumulation

of proteostatic load in a given mitochondrial compartment leads to localized activation of mitophagy receptors, leading to selective degradation of mitochondrial compartments enriched in specific protein species. This outlines a model in which protein lesions lead to changes in posttranslational modifications of the damaged molecules, which lead in turn to these proteins being concentrated into discrete compartments that are targeted for mitophagic degradation (Figure 10). Regulation of phase partitioning of proteins by phosphorylation has precedents: the regulation of RNA granule formation in the cytosol (Thomas *et al*., 2011; Kedersha *et al*., 2016; Panas *et al*., 2016) and milk globule formation (Bijl *et al*., 2014) are two well-studied examples.

Such a model, where fission and fusion play an indirect role in mitophagy, would reconcile a number of apparently contradictory results in the literature. Many publications have claimed that mitochondrial fission is essential for mitophagy (Gomes and Scorrano, 2008, 2013; Kageyama *et al*., 2014; Mishra and Chan, 2014). However, most of these posit a direct mechanistic role, either in generating 'bite sized' engulfable fragments and some even imply a molecular interaction between the autophagic machinery and the fission machinery (Mao *et al*., 2013). In contrast, a recent publication claimed that mitochondrial fission mediated by Drp1/Dnm1 is completely unnecessary for mitophagy (Yamashita *et al*., 2016), and that the autophagic machinery itself mediates fission during engulfment. A model in which mitochondrial dynamics has no role whatsoever does not explain the reproducible slowdown of mitophagy in *dnm1Δ* cells, which was repeatedly observed in multiple publications from different groups (Kanki et al, 2008; Abeliovich et al, 2013; Yamashita *et al*., 2016). However it is perfectly consistent with a 'percolation' or 'distillation' role of mitochondrial dynamics, in determining the selectivity and rate of mitophagy, as we have proposed (Abeliovich *et al*., 2013; Dengjel and Abeliovich, 2014).

An alternative hypothesis would be to postulate that specific protein-protein interactions regulate the segregation of proteins into mitophagy-bound compartments. This type of model must address several difficult questions. Are all mitochondrial proteins interacting with a small subset of proteins which function promiscuously to mediate mitophagic selectivity? Surely one cannot have each mitochondrial matrix protein surveilled by a different and unique mitophagy regulator? We currently favor the nonspecific, phase separation model, as it imposes fewer constraints on the system and requires fewer assumptions. However, further studies must be carried out before one of these hypotheses is ruled out.

In summary, our results suggest a potential mechanism for generating mitophagic selectivity at the molecular level, and indicate a role for protein phosphorylation in regulating mitophagic trafficking of individual mitochondrial matrix protein molecules.

Materials and Methods

Plasmids

The plasmids and oligonucleotides used in this study are listed in Supplementary Tables III and IV, respectively. To make plasmids PKB1 and PKB2, the *AUP1* reading frame full length and an alternative insert lacking 34 amino acids from the N-terminal of the reading frame, respectively, were amplified using a PCR reaction. The primers P1 (5'-ATACTAACTAGTTACAACATGCGGCTGGGGAATCT ATG-3') and P2 (5'-ATACTAATCGATTTAGTTTAATTTTGTTTCGTTAGATTG-3) contain *ClaI* and *SpeI* linkers (supplementary table III). The PCR product was digested then with *ClaI* and *SpeI* and ligated into a *ClaI* and *SpeI* digested pCU416. To construct plasmid PKB32, the Mdh1-GFP open reading frame (ORF) was amplified by HAY840 yeast genomic DNA using a PCR reaction and oligonucleotides primers P7 Forward: 5'-ATACTAACTAGTTACAACA TGTTGTCAAGAGTAGCTAAAC-3' and P8 Reverse: 5'-ATACTAATCGATGACCTCATACTATACCTG-3' containing *ClaI* and *SpeI* restriction sites (supplementary table IV). The PCR product was digested with *ClaI-SpeI* and ligated into a *ClaI* and *SpeI* digested pCU416, generating a fusion protein under the control of the *CUP1* promoter. Plasmid PKB65 was generated by cloning the Mdh1-GFP reading frame, together with 800 bases of 5' and 500 bases of 3' sequences was amplified using a PCR and primers P5 Forward: 5'-ATACTAGGATCCC AAAAGATCGACGCAATG-3' and P6 Reverse: 5'-ATACTAGAGCTCGACCTCATACTATACCTG-3' (table 4) containing *BamHI* and *SacI* linkers. The PCR product was digested with *BamHI-SacI* and ligated into a *BamHI-SacI* digested pRS415. All the plasmids were verified by sequencing (Hylabs, Rehovot).

Yeast strains and growth conditions

Yeast strains used in this study are listed in Supplementary Table II. Deletion mutants and epitope-tagged strains were conducted by the cassette integration method (Longtine *et al*., 1998). Strain HAY75 (MATα *leu2-3,112 ura3-52 his3-Δ200 trp1-Δ901 lys2-801 suc2-Δ9*) was used as the WT genetic background in this study. For primers details, see supplementary table IV.

All knockout strains were verified by PCR. Oligonucleotides used in this study are detailed in Supplementary Table IV.

Yeast were grown in synthetic dextrose medium (0.67% yeast nitrogen base w/o amino acids (Difco), 2% glucose, auxotrophic requirements and vitamins as required) or in SL medium (0.67% yeast nitrogen base w/o amino acids (Difco), 2% lactate pH 6, 0.1% glucose, auxotrophic requirements and vitamins as required). All culture growth and manipulation were at 26 ^{0}C. Yeast transformation was according to Gietz and Woods (Gietz and Woods, 2002).

For nitrogen starvation experiments, cells were grown to mid-log phase (OD_{600} of 0.4-0.6) in synthetic dextrose medium (SD), washed with distilled water, and resuspended in nitrogen starvation medium (0.17 YNB-N (Difco), 2% glucose) for the times indicated in individual experiments. Overexpression studies with *CUP1* promoter-based vectors were carried out by supplementing the medium with 5 μM $CuSO_4$, for both control (empty vector) and overexpressing cells.

Chemicals and antisera

Chemicals were purchased from Sigma-Aldrich (Rehovot, Israel) unless otherwise stated. Custom oligonucleotides were from Hylabs (Rehovot, Israel). Anti-GFP antiserum was from Santa-Cruz (Dallas, TX). Horseradish peroxidase-conjugated goat anti-rabbit antibodies were from MP Biomedicals (Santa Ana, CA).

Fluorescence microscopy

Culture samples (3 μl) were placed on standard microscope slides and viewed using a Nikon Eclipse E600 fluorescence microscope equipped with the appropriate filters and a Photometrics Coolsnap HQ CCD. To achieve statistically significant numbers of cells per viewing field in the pictures, 1 ml cells were collected and centrifuged for 1 min at 3,500 xg. For quantitative analysis of co-localization, ImageJ software with the co-localization Plugin, JACoP (Bolte and Cordelières, 2006). Representative fields were analyzed in terms of channel intensity correlation coefficient. For quantitative estimates of mitophagic trafficking, mitophagy, was scored as the appearance fluorescent proteins in the vacuolar lumen. For statistical analysis, ANOVA analysis was carried out using JMP 12 software. Correlations were compared over mutations and days by two-factor ANOVA. As the mutation X day interaction effect was statistically significant ($p<0.0001$), the two days were compared for each mutation by contrast t-tests. Pre-planned comparisons to WT were also performed by contrast t-tests. For confocal microscopy**,** cells were placed on standard microscope slides and micrographs were obtained by confocal laser scanning microscopy using a Leica SP8, using a 63x water immersion lens. GFP excitation was carried out using the 488 nm line, and emission was collected between 500-540 nm. For

RFP excitation we used the 552 nm line and fluorescence emission was collected between 590-640 nm. GFP and RFP co-localization images were acquired using LasAF software and the images were analyzed by Fiji software.

Preparation of whole-cell extracts for western blot analysis

Cells (10 OD_{600} units) were treated with 10% cold trichloroacetic acid (TCA) and washed three times with cold acetone. The dry cell pellet was then resuspended in 100 µl cracking buffer (50 mM Tris pH 6.8, 6 M urea, 1 mM EDTA, 1% SDS) and vortexed in Tomy MT-360 microtube mixer at maximum speed, with an equal volume of acid-washed glass beads (425-600 µm diameter), for a total of 30 min. Lysates were clarified by centrifugation at 17,000 xg for 5 min and total protein was quantified in the supernatant using the BCA protein assay (Thermo Scientific, Rockford, IL). SDS loading buffer (final concentrations of 100 mM Tris pH 6.8, 20% glycerol, 2% SDS, 500 mM β-mercaptoethanol) was added to the lysate and the samples were warmed to 60°C for 5 min prior to loading on gels. ImageJ software was used for band quantification.

Immunoblotting

SDS-10% polyacrylamide gels were transferred to nitrocellulose membrane by using either a wet or semidry blotting transfer system. Membranes were blocked for 1 h with TPBS (137 mM NaCl, 2.7 mM KCL, 10 mM Na_2HPO_4, 1.8 mM KH_2PO_4, 1 % Tween and 5 % milk powder (BD Difco Skim Milk), followed by incubation with anti-GFP rabbit (1:5000) for 1.5 h, then washed 4x 2 min with TPBS, incubated for 1.5 h with HRP conjugated secondary antibody (1:10000). The membranes were then washed 4x with TPBS, incubated with SuperSignal Chemiluminescence substrate (Thermo Scientific), and exposed to Molecular Imager ChemiDoc™ XRS imaging system. Where necessary, 2% normal goat serum was added to reduce background.

Native immunoprecipitation.

Cells (20 OD_{600} units) were washed 3x with 1 ml of cold 10 mM PIPES pH 7, 2 mM PMSF. The cell pellet was washed in three volumes of cold lysis buffer (20 mM HEPES pH 7.4, 50 mM NaCl, 1mM EDTA, 10% glycerol, 0.2 mM $NaOV_4$, 10 mM $NaPO_4$, 10 mM β-glycerophosphate, 10 mM NaF, 10% phosphate cocktail inhibitors, 1 mM PMSF, proteases inhibitors (final concentrations: 5 µg/ ml

antipain, 1 µg/ml aprotinin, 0.5 µg/ml leupeptin, 0.7 µg/ml pepstatin). The cells were then frozen in liquid nitrogen and stored at -80°C. Extracts were prepared from the frozen pellets using a SPEX Freezer/Mill according to the manufacturer's instruction. The frozen ground yeast powder was thawed at room temperature, and equal amount of lysis buffer plus Triton-X100 was added to a final concentration of 0.5% v/v detergent. Cell debris was removed by centrifugation at 17.000x g for 10 min at 4°C. 20 µl of GFP-Trap bead slurry (Chromotek) was pre-equilibrated in lysis buffer, per the manufacturer's instructions. The cleared lysate was added to the equilibrated beads and incubated for 1 h at 4 °C with constant mixing. The beads were washed five times with 1 ml ice cold wash buffer (20 mM HEPES pH 7.4, 50 mM NaCl, 0.5 mM EDTA, 10% glycerol, 0.5% Triton-X, 0.2 mM $NaOV_3$, 10 mM $NaPO_3$, 10 mM β-glycerophosphate, 10 mM NaF, resuspended in 50 µl 2x SDS-loading buffer (200 mM Tris pH 6.8, 40% glycerol, 4% SDS, 1 M β-mercaptoethanol) and boiled for 10 min at 95°C. For phosphatase treatment, immunoprecipitated beads were incubated with 40 Units of lambda protein phosphate (New England Biolabs) in a 50 µl reaction. Samples were washed once with wash buffer and resuspended in 50 µl 2 x SDS-loading buffer.

SILAC labeling

To quantify relative phosphorylation on amino acid residues in Mdh1-GFP in *AUP1* and *aup1Δ* backgrounds, cell cultures of each strain were grown separately in SL medium supplemented respectively with 0.003% (w/v) $^{13}C_6$ $^{15}N_2$L-lysine (Lys8; Cat. Number 211604102, Silantes, Munich) and 0.001% (w/v) $^{13}C_6{}^{15}N_4$ L-arginine (Arg10; Cat. Number 201603902, Silantes, Munich) or with identical concentrations of unlabeled lysine and arginine, in addition to the standard auxotrophy supplementation. At each time point, 50 OD_{600} units of cells from each labeling regime were combined, washed with cold lysis buffer, and frozen in liquid nitrogen and processed for native immunoprecipitation as described in the previous section. Phosphopeptide ratios were normalized to respective Mdh1-GFP ratios.

MS analysis

Mass spectrometric measurements were performed on a Q Exactive Plus mass spectrometer coupled to an EasyLC 1000 (Thermo Fisher Scientific, Bremen, Germany). Prior to analysis phosphopeptides were enriched by TiO_2 , as described previously (Rigbolt *et al*., 2014). The MS raw data files were

analysed by the MaxQuant software (Cox and Mann, 2008) version 1.4.1.2, using a Uniprot *Saccharomyces cerevisiae* database from March 2016 containing common contaminants such as keratins and enzymes used for in-gel digestion.

Site directed mutagenesis

Site directed mutagenesis protocol was carried out according to the Stratagene QuikChange system. *Pfu* DNA Polymerase (Fermentas) was used with a thermocycling protocol followed by removal of the parental strands with *DpnI* digestion. Thermocycling conditions were as follows: Initial denaturation at 95°C for 2 min, then (steps 2-4), 30 sec at 95°C, 60 sec at 55°C, and 12 min at 68 °C. Steps 2-4 repeated for 18 cycles. PCR products were treated with DpnI (fermentas) for 1 hr at 37°C, and precipitated using with 70% ethanol. DNA pellets were then dried and resuspended with 20 µl TE buffer pH 8. All mutagenesis products were transformed into *E. coli* DH5α, and mutations were verified by sequencing. The oligonucleotide primers used to create site-directed MDH1-GFP variants and combined variants are listed in Supplementary Table III.

Cell fractionation

Cells (20 OD_{600} units) were collected by centrifugation at 3,500 xg, 5 min, 4°C. The cells were spheroplasted in medium containing 1 M sorbitol and 0.6 mg/ml zymolyase (0.67 % yeast nitrogen base, 2 % glucose, auxotrophic requirements and vitamins as required, 1 M sorbitol, 40 mM HEPES pH 7, 0.6 mg/ml zymolase) for 30 min at 37°C. Spheroplasts were collected by centrifugation at 200xg g for 5 min. The spheroplasts were resuspended on ice in lysis buffer (0.2 M sorbitol, 50 mM potassium acetate, 2 mM EDTA, 40 mM HEPES pH 7, plus proteases inhibitors), transferred to a pre-cooled dounce homogenizer and dounced 15 times with a tight fitting pestle. The lysate was then transferred to eppendorf tubes and centrifuged at 300 xg, 4°C, 5 min. 1 ml of cleared supernatant was saved as total extract fraction (T). The rest was transferred to clean eppendorf tubes and centrifuged at 13.000x g, 10 min, 4°C. 1 ml of the supernatant was labeled as S13 (cytosolic proteins). The pellet was labeled as P13. The S13 and total extract fractions (1 ml each) were precipitated with 10% cold TCA by adding 500 µl of 30% TCA, while the P13 fraction was first resuspended in 1 ml lysis buffer and then

precipitated with 10 % TCA. For immunoblot analysis, 0.5 OD_{600} equivalents were loaded per lane on SDS-PAGE gels.

Generation of selectivity profile comparisons and heat maps

To compare between different genotypes, % free GFP values which were recorded from immunoblots of Mdh1-GFP, Aco1-GFP, Aco2-GFP, Qcr2-GFP and Idp1-GFP were normalized, such that each value of % free GFP was divided by the average value of all % free GFP measured for the same protein over all genotypes. This centered the data distribution such that all proteins contributed equally to the correlation calculation. Normalized data points of 3 biological replicates were averaged. We then calculated a Pearson correlation value (r (correlation coefficient) and p – values (significance of correlation) between all phenotype pairs (vector of normalized averaged % free GFP per protein) using the rcorr function in R (Hmisc package). A heat map was generated using the heatmap.2 function in R (gplots package). The heat map cells contains the r correlation measured and colored from negative correlation in red to positive correlation in yellow.

The dendogram was generated by calculating the Euclidean distance measure between correlation vectors of each genotype using the complete linkage method.

Acknowledgements

We wish to thank Chris Meisinger and Corvin Walter for advice on mitochondrial protein phosphorylation, Hillary Voet and Inbar Plaschkes for help with statistical analysis, Einat Zelinger for help with confocal microscopy, and J.C. Martinou for discussions. This work was funded by ISF grant 422/12 (to HA), ISF grant 445/17 (to HA), GIF grant I-111-412.7-2014 (to HA and JD), the Swiss National Science Foundation, grant 31003A-166482/1, and TRANSAUTOPHAGY, COST Action CA15138 (to JD).

Author contributions

P.K. carried out experiments, generated SILAC-labeled samples for MS analysis, and wrote the manuscript. M.R. and J.Z. carried out MS analyses, and analyzed the MS data. J.D. carried out analyses of MS data, planned experiments and wrote the manuscript. H.A. planned experiments and wrote the manuscript.

Conflict of Interest

The authors declare no conflict of interest

References

1. Abeliovich H, Dengjel J (2016) Mitophagy as a stress response in mammalian cells and in respiring S. cerevisiae. *Biochem Soc Trans*, **44:** 541–545
2. Abeliovich H, Zarei M, Rigbolt KT, Youle RJ, Dengjel J (2013) Involvement of mitochondrial dynamics in the segregation of mitochondrial matrix proteins during stationary phase mitophagy. *Nat Commun*, **4:** 2789
3. Aoki Y, Kanki T, Hirota Y, Kurihara Y, Saigusa T, Uchiumi T, Kang D (2011) Phosphorylation of Ser114 on Atg32 mediates mitophagy. *Mol Biol Cell*, 22(17):3206–17
4. Banerjee K, Munshi S, Xu H, Frank DE, Chen HL, Chu CT, Yang J, Cho S, Kagan VE, Denton TT, Tyurina YY, Jiang JF, Gibson GE (2016) Mild mitochondrial metabolic deficits by α-ketoglutarate dehydrogenase inhibition cause prominent changes in intracellular autophagic signaling: Potential role in the pathobiology of Alzheimer's disease. *Neurochem Int*, **96:** 32–45
5. Bijl E, van Valenberg HJ, Huppertz T, van Hooijdonk AC, Bovenhuis H (2014) Phosphorylation of αS1-casein is regulated by different genes. *J Dairy Sci*, **97:** 7240–7246
6. Bolte S, Cordelières FP (2006) A guided tour into subcellular colocalization analysis in light microscopy. *J Microsc*, **224:** 213–232
7. Bratic A, Larsson NG (2013) The role of mitochondria in aging. *J Clin Invest*, **123:** 951–957
8. Burman JL, Pickles S, Wang C, Sekine S, Vargas JNS, Zhang Z, Youle AM, Nezich CL, Wu X, Hammer JA, Youle RJ (2017) Mitochondrial fission facilitates the selective mitophagy of protein aggregates. *J Cell Biol*,
9. Corsetti V, Florenzano F, Atlante A, Bobba A, Ciotti MT, Natale F, Della Valle F, Borreca A, Manca A, Meli G, Ferraina C, Feligioni M, D'Aguanno S, Bussani R, Ammassari-Teule M, Nicolin V, Calissano P, Amadoro G (2015) NH2-truncated human tau induces deregulated mitophagy in neurons by aberrant recruitment of Parkin and UCHL-1: implications in Alzheimer's disease. *Hum Mol Genet*, **24:** 3058–3081
10. Cox J, Mann M (2008) MaxQuant enables high peptide identification rates, individualized p.p.b.-range mass accuracies and proteome-wide protein quantification. *Nat Biotechnol*, **26:** 1367–1372
11. Dengjel J, Abeliovich H (2014) Musical chairs during mitophagy. *Autophagy*, **10:** 706–707
12. Dengjel J, Abeliovich H (2016) Roles of mitophagy in cellular physiology and development. *Cell Tissue Res*,
13. Diot A, Morten K, Poulton J (2016) Mitophagy plays a central role in mitochondrial ageing. *Mamm Genome*, **27:** 381–395
14. Esteban-Martínez L, Sierra-Filardi E, McGreal RS, Salazar-Roa M, Mariño G, Seco E, Durand S, Enot D, Graña O, Malumbres M, Cvekl A, Cuervo AM, Kroemer G, Boya P (2017) Programmed mitophagy is essential for the glycolytic switch during cell differentiation. *EMBO J*,
15. Farré JC, Burkenroad A, Burnett SF, Subramani S (2013) Phosphorylation of mitophagy and pexophagy receptors coordinates their interaction with Atg8 and Atg11. *EMBO Rep*, **14:** 441–449
16. Gey U, Czupalla C, Hoflack B, Rödel G, Krause-Buchholz U (2008) Yeast pyruvate dehydrogenase complex is regulated by a concerted activity of two kinases and two phosphatases. *J Biol Chem*, **283:** 9759–9767
17. Gietz RD, Woods RA (2002) Transformation of yeast by lithium acetate/single-stranded carrier DNA/polyethylene glycol method. *Methods Enzymol*, **350:** 87–96
18. Goldstein AL, McCusker JH (1999) Three new dominant drug resistance cassettes for gene disruption in Saccharomyces cerevisiae. *Yeast*, **15:** 1541–1553
19. Gomes LC, Scorrano L (2008) High levels of Fis1, a pro-fission mitochondrial protein, trigger autophagy. *Biochim Biophys Acta*, **1777:** 860–866
20. Gomes LC, Scorrano L (2013) Mitochondrial morphology in mitophagy and macroautophagy. *Biochim Biophys Acta*, **1833:** 205–212

21. González A, Casado C, Ariño J, Casamayor A (2013) Ptc6 is required for proper rapamycin-induced down-regulation of the genes coding for ribosomal and rRNA processing proteins in S. cerevisiae. *PLoS One*, **8:** e64470
22. Green DR, Galluzzi L, Kroemer G (2011) Mitochondria and the Autophagy-Inflammation-Cell Death Axis in Organismal Aging. *Science*, **333:** 1109–1112
23. Guo X, Sun X, Hu D, Wang YJ, Fujioka H, Vyas R, Chakrapani S, Joshi AU, Luo Y, Mochly-Rosen D, Qi X (2016) VCP recruitment to mitochondria causes mitophagy impairment and neurodegeneration in models of Huntington's disease. *Nat Commun*, **7:** 12646
24. Hämäläinen RH, Manninen T, Koivumäki H, Kislin M, Otonkoski T, Suomalainen A (2013) Tissue- and cell-type-specific manifestations of heteroplasmic mtDNA 3243A>G mutation in human induced pluripotent stem cell-derived disease model. *Proc Natl Acad Sci U S A*, **110:** E3622–30
25. Holt LJ, Tuch BB, Villén J, Johnson AD, Gygi SP, Morgan DO (2009) Global analysis of Cdk1 substrate phosphorylation sites provides insights into evolution. *Science*, **325:** 1682–1686
26. Kageyama Y, Hoshijima M, Seo K, Bedja D, Sysa-Shah P, Andrabi SA, Chen W, Höke A, Dawson VL, Dawson TM, Gabrielson K, Kass DA, Iijima M, Sesaki H (2014) Parkin-independent mitophagy requires Drp1 and maintains the integrity of mammalian heart and brain. *EMBO J*, **33:** 2798–2813
27. Kane LA, Lazarou M, Fogel AI, Li Y, Yamano K, Sarraf SA, Banerjee S, Youle RJ (2014) PINK1 phosphorylates ubiquitin to activate Parkin E3 ubiquitin ligase activity. *J Cell Biol*, **205:** 143–153
28. Kanki T, Furukawa K, Yamashita S (2015) Mitophagy in yeast: Molecular mechanisms and physiological role. *Biochim Biophys Acta*, **1853:** 2756–2765
29. Kanki T, Wang K, Cao Y, Baba M, Klionsky DJ (2009) Atg32 is a mitochondrial protein that confers selectivity during mitophagy. *Dev Cell*, **17:** 98–109
30. Kazlauskaite A, Kondapalli C, Gourlay R, Campbell DG, Ritorto MS, Hofmann K, Alessi DR, Knebel A, Trost M, Muqit MM (2014) Parkin is activated by PINK1-dependent phosphorylation of ubiquitin at Ser65. *Biochem J*, **460:** 127–139
31. Kedersha N, Panas MD, Achorn CA, Lyons S, Tisdale S, Hickman T, Thomas M, Lieberman J, McInerney GM, Ivanov P, Anderson P (2016) G3BP-Caprin1-USP10 complexes mediate stress granule condensation and associate with 40S subunits. *J Cell Biol*, **212:** 845–860
32. Kinoshita-Kikuta E, Aoki Y, Kinoshita E, Koike T (2007) Label-free kinase profiling using phosphate affinity polyacrylamide gel electrophoresis. *Mol Cell Proteomics*, **6:** 356–366
33. Klionsky DJ et al. (2012) Guidelines for the use and interpretation of assays for monitoring autophagy. *Autophagy*, **8:** 445–544
34. Kondapalli C, Kazlauskaite A, Zhang N, Woodroof HI, Campbell DG, Gourlay R, Burchell L, Walden H, Macartney TJ, Deak M, Knebel A, Alessi DR, Muqit MM (2012) PINK1 is activated by mitochondrial membrane potential depolarization and stimulates Parkin E3 ligase activity by phosphorylating Serine 65. *Open Biol*, **2:** 120080
35. Koyano F, Okatsu K, Kosako H, Tamura Y, Go E, Kimura M, Kimura Y, Tsuchiya H, Yoshihara H, Hirokawa T, Endo T, Fon EA, Trempe JF, Saeki Y, Tanaka K, Matsuda N (2014) Ubiquitin is phosphorylated by PINK1 to activate parkin. *Nature*, **510:** 162–166
36. Krause-Buchholz U, Gey U, Wünschmann J, Becker S, Rödel G (2006) YIL042c and YOR090c encode the kinase and phosphatase of the Saccharomyces cerevisiae pyruvate dehydrogenase complex. *FEBS Lett*, **580:** 2553–2560
37. Lazarou M, Sliter DA, Kane LA, Sarraf SA, Wang C, Burman JL, Sideris DP, Fogel AI, Youle RJ (2015) The ubiquitin kinase PINK1 recruits autophagy receptors to induce mitophagy. *Nature*, **524:** 309–314
38. Longtine MS, McKenzie A, Demarini DJ, Shah NG, Wach A, Brachat A, Philippsen P, Pringle JR (1998) Additional modules for versatile and economical PCR-based gene deletion and modification in Saccharomyces cerevisiae. *Yeast*, **14:** 953–961
39. Mao K, Wang K, Liu X, Klionsky DJ (2013) The scaffold protein Atg11 recruits fission machinery to drive selective mitochondria degradation by autophagy. *Developmental cell*, **26:** 9–18
40. Mishra P, Chan DC (2014) Mitochondrial dynamics and inheritance during cell division, development and disease. *Nat Rev Mol Cell Biol*, **15:** 634–646

41. Mortensen M, Ferguson DJ, Edelmann M, Kessler B, Morten KJ, Komatsu M, Simon AK (2010) Loss of autophagy in erythroid cells leads to defective removal of mitochondria and severe anemia in vivo. *Proc Natl Acad Sci U S A*, **107:** 832–837
42. Narendra D, Tanaka A, Suen DF, Youle RJ (2008) Parkin is recruited selectively to impaired mitochondria and promotes their autophagy. *J Cell Biol*, **183:** 795–803
43. Narendra DP, Jin SM, Tanaka A, Suen DF, Gautier CA, Shen J, Cookson MR, Youle RJ (2010) PINK1 is selectively stabilized on impaired mitochondria to activate Parkin. *PLoS Biol*, **8:** e1000298
44. Narendra DP, Youle RJ (2011) Targeting mitochondrial dysfunction: role for PINK1 and Parkin in mitochondrial quality control. *Antioxid Redox Signal*, **14:** 1929–1938
45. Novak I, Kirkin V, McEwan DG, Zhang J, Wild P, Rozenknop A, Rogov V, Löhr F, Popovic D, Occhipinti A, Reichert AS, Terzic J, Dötsch V, Ney PA, Dikic I (2010) Nix is a selective autophagy receptor for mitochondrial clearance. *EMBO Rep*, **11:** 45–51
46. Okamoto K, Kondo-Okamoto N, Ohsumi Y (2009) Mitochondria-anchored receptor Atg32 mediates degradation of mitochondria via selective autophagy. *Dev Cell*, **17:** 87–97
47. Ordureau A, Sarraf SA, Duda DM, Heo JM, Jedrychowski MP, Sviderskiy VO, Olszewski JL, Koerber JT, Xie T, Beausoleil SA, Wells JA, Gygi SP, Schulman BA, Harper JW (2014) Quantitative proteomics reveal a feedforward mechanism for mitochondrial PARKIN translocation and ubiquitin chain synthesis. *Mol Cell*, **56:** 360–375
48. Panas MD, Ivanov P, Anderson P (2016) Mechanistic insights into mammalian stress granule dynamics. *J Cell Biol*, **215:** 313–323
49. Papa S, Scacco S, De Rasmo D, Signorile A, Papa F, Panelli D, Nicastro A, Scaringi R, Santeramo A, Roca E, Trentadue R, Larizza M (2010) cAMP-dependent protein kinase regulates post-translational processing and expression of complex I subunits in mammalian cells. *Biochim Biophys Acta*, **1797:** 649–658
50. Pickrell AM, Youle RJ (2015) The roles of PINK1, parkin, and mitochondrial fidelity in Parkinson's disease. *Neuron*, **85:** 257–273
51. Reinders J, Wagner K, Zahedi RP, Stojanovski D, Eyrich B, van der Laan M, Rehling P, Sickmann A, Pfanner N, Meisinger C (2007) Profiling phosphoproteins of yeast mitochondria reveals a role of phosphorylation in assembly of the ATP synthase. *Mol Cell Proteomics*, **6:** 1896–1906
52. Renvoisé M, Bonhomme L, Davanture M, Valot B, Zivy M, Lemaire C (2014) Quantitative variations of the mitochondrial proteome and phosphoproteome during fermentative and respiratory growth in Saccharomyces cerevisiae. *J Proteomics*, **106:** 140–150
53. Rigbolt KT, Zarei M, Sprenger A, Becker AC, Diedrich B, Huang X, Eiselein S, Kristensen AR, Gretzmeier C, Andersen JS, Zi Z, Dengjel J (2014) Characterization of early autophagy signaling by quantitative phosphoproteomics. *Autophagy*, **10:** 356–371
54. Sandoval H, Thiagarajan P, Dasgupta SK, Schumacher A, Prchal JT, Chen M, Wang J (2008) Essential role for Nix in autophagic maturation of erythroid cells. *Nature*, **454:** 232–235
55. Shiba-Fukushima K, Imai Y, Yoshida S, Ishihama Y, Kanao T, Sato S, Hattori N (2012) PINK1-mediated phosphorylation of the Parkin ubiquitin-like domain primes mitochondrial translocation of Parkin and regulates mitophagy. *Sci Rep*, **2:** 1002
56. Sin J, Andres AM, Taylor DJ, Weston T, Hiraumi Y, Stotland A, Kim BJ, Huang C, Doran KS, Gottlieb RA (2016) Mitophagy is required for mitochondrial biogenesis and myogenic differentiation of C2C12 myoblasts. *Autophagy*, **12:** 369–380
57. Steensma HY, Tomaska L, Reuven P, Nosek J, Brandt R (2008) Disruption of genes encoding pyruvate dehydrogenase kinases leads to retarded growth on acetate and ethanol in Saccharomyces cerevisiae. *Yeast*, **25:** 9–19
58. Swaney DL, Beltrao P, Starita L, Guo A, Rush J, Fields S, Krogan NJ, Villén J (2013) Global analysis of phosphorylation and ubiquitylation cross-talk in protein degradation. *Nat Methods*, **10:** 676–682
59. Tal R, Winter G, Ecker N, Klionsky DJ, Abeliovich H (2007) Aup1p, a yeast mitochondrial protein phosphatase homolog, is required for efficient stationary phase mitophagy and cell survival. *J Biol Chem*, **282:** 5617–5624

60. Thomas MG, Loschi M, Desbats MA, Boccaccio GL (2011) RNA granules: the good, the bad and the ugly. *Cell Signal*, **23:** 324–334
61. Torggler R, Papinski D, Kraft C (2017) Assays to Monitor Autophagy in Saccharomyces cerevisiae. *Cells*, **6:**
62. Twig G, Elorza A, Molina AJ, Mohamed H, Wikstrom JD, Walzer G, Stiles L, Haigh SE, Katz S, Las G, Alroy J, Wu M, Py BF, Yuan J, Deeney JT, Corkey BE, Shirihai OS (2008) Fission and selective fusion govern mitochondrial segregation and elimination by autophagy. *EMBO J*, **27:** 433–446
63. Vélot C, Lebreton S, Morgunov I, Usher KC, Srere PA (1999) Metabolic effects of mislocalized mitochondrial and peroxisomal citrate synthases in yeast Saccharomyces cerevisiae. *Biochemistry*, **38:** 16195–16204
64. von der Malsburg K et al. (2011) Dual role of mitofilin in mitochondrial membrane organization and protein biogenesis. *Dev Cell*, **21:** 694–707
65. Wang K, Jin M, Liu X, Klionsky DJ (2013) Proteolytic processing of Atg32 by the mitochondrial i-AAA protease Yme1 regulates mitophagy. *Autophagy*, **9:** 1828–1836
66. Yamashita SI, Jin X, Furukawa K, Hamasaki M, Nezu A, Otera H, Saigusa T, Yoshimori T, Sakai Y, Mihara K, Kanki T (2016) Mitochondrial division occurs concurrently with autophagosome formation but independently of Drp1 during mitophagy. *J Cell Biol*, **215:** 649–665

Figure legends

Figure 1. **Aup1 is required for mitophagic trafficking of Mdh1-GFP expressed from its endogenous promoter**. WT and *aup1Δ* cells, harboring different pCU416-derived plasmids as indicated, were grown on SL medium for the indicated times, as described in "Materials and Methods". The cells were then harvested and the corresponding protein extracts were immunoblotted with anti-GFP antibody. A) deletion of *AUP1* blocks mitophagic trafficking of Mdh1-GFP, and expression of the full Aup1 reading frame from a plasmid-based *CUP1* promoter overcomes this block. Note that truncation of the putative mitochondrial targeting sequence (*aup1Δ34*) of Aup1 prevents the rescue. B. Control demonstrating that mitophagic trafficking of integrated Mdh1-GFP is absolutely dependent on the Atg32 receptor protein. Blots are representative of at least 3 independent biological replicates.

Figure 2. Overexpression of reporter proteins suppresses the requirement for Aup1. WT and *aup1Δ* cells overexpressing Mdh1-GFP (A) or Idp1-GFP (C) from a plasmid-borne *CUP1* promoter were grown on SL medium for the indicated times, as described in "Materials and Methods". The cells were then harvested and the corresponding protein extracts were immunoblotted with anti-GFP

antibody. (B) and (D); WT and *aup1Δ* cells expressing (B) Mdh1-GFP or Idp1-GFP (D) from the respective endogenous promoters were grown on SL medium for the indicated times, as described in "Materials and Methods". The cells were then harvested and the corresponding protein extracts were immunoblotted with anti-GFP antibody. Blots are representative of at least 3 independent biological replicates.

Figure 3. Mitochondrial kinases and phosphatases regulate the selectivity of mitophagy. **A.** A 5x6 matrix of WT, *aup1Δ*, *ptc5Δ*, *pkp1Δ*, *pkp2Δ* and pkp1*Δ* *pkp2Δ* cells, each expressing, respectively, Aco1-GFP, Qcr2-GFP, Aco1-GFP, Mdh1-GFP and Idp1-GFP from the respective native promoters was assayed for release of free GFP by immunoblotting after a 5 day incubation in SL medium as described in "Materials and Methods". Free GFP was quantified by densitometry and normalized as percent of the total GFP signal (free GFP + chimera) in the respective lanes. Bars denote standard deviation (N=3, 2-way ANOVA, $P=1x10^{-17}$). For statistical significance of individual pairwise comparisons, see Supplementary Table I. **B.** Pearson correlation coefficients and clustering analysis for the normalized selectivity vectors (see Supplementary Figure 2) defined by each of the single mutant genotypes tested in **A** (see Materials and Methods for details).

Figure 4. **Mdh1-GFP is phosphorylated under mitophagy-inducing conditions**.
Extracts from TVY1 cells grown in SL medium for 1 day were digested, phosphopeptide-enriched and analysed by LC-MS/MS for the detection of Mdh1-derived phosphopeptides**. (A**) Serine 240, **(B)** Thr199 and **(C)** Ser196 of Mdh1-GFP are phosphorylated during growth in SL.

Figure 5. Serine/threonine to alanine mutagenesis of known phosphosites on Mdh1 affects the selective mitophagy of Mdh1-GFP without blocking overall mitophagy. (A) PKY365 cells harboring plasmids expressing different Mdh1-GFP variants from the endogenous *MDH1* promoter were incubated in SL medium for 1 or 5 days as indicated and protein extracts were prepared. Equal amounts of protein (20 μg) were subjected to SDS-PAGE and immunoblotting with anti-GFP antibody. The % free GFP was normalized to WT, for each variant. Error bars indicate S.E. (N=3). **(B) Point mutations in Mdh1-GFP prevent mitophagic trafficking of the specific reporter, but do not affect mitophagic trafficking of a co-expressed mtRFP reporter**. Cells (PKY365) expressing WT Mdh1-GFP and the indicated variants from the native *MDH1* promoter together with a mitochondrially

targeted mtRFP were incubated in SL medium for 5 days and imaged by fluorescence microscopy. WT MDH1-GFP shows mitophagic targeting (white arrows) by day 5, which co-localizes with the mtRFP signal in these cells. In contrast, the mutants show defective routing to the vacuole, while the RFP signal in the vacuole is not affected (white arrows). Scale bar = 1 μm. **(C) The difference between point mutants of Mdh1 cannot be explained by differential sensitivity to vacuolar proteases, and depends on mitochondrial targeting**. WT (HAY75), *atg32Δ*, and *atg1Δ* cells expressing truncated versions of MDH1 lacking the mitochondrial targeting sequence were subjected to nitrogen starvation for 12 h to induce macroautophagy, and protein extracts were analyzed by immunoblotting. The two left-most lanes are control cells expressing full length WT and T199A versions of Mdh1, which were subjected to the standard 5 day stationary phase mitophagy protocol, for comparison (N=3). **(D) Serine/threonine to aspartate mutagenesis of T199 and S240 on Mdh1 leads to reciprocal effects on Mdh1-GFP mitophagic trafficking, relative to the respective alanine mutations.** PKY365 cells transformed with vectors expressing Mdh1-GFP and the indicated variants from the endogenous *MDH1* promoter, were incubated in SL medium for 1 or 5 days, and protein extracts were prepared. Equal amounts of protein (20 μg) were subjected to SDS-PAGE and immunoblotting with anti-GFP antibody. The % free GFP was normalized to WT, for each variant. Error bars indicate s.d, analysis of variation of three independent experiments (N=3).

Figure 6. Dynamic changes in Mdh1-GFP phosphorylation state occur during stationary phase mitophagy.

(A) Anti-phosphoamino acid immunoblotting of anti-GFP immunoprecipitates demonstrate the effects of *AUP1* deletion on Mdh1-GFP phosphorylation. PKY395 (*aup1Δ*) and control TVY1 cells, both expressing Mdh1-GFP, were grown in SL medium. At the indicated time points, protein extracts were generated under native conditions and immunoprecipitated with anti-GFP antibodies as detailed in "Materials and Methods". The immunoprecipitates were analyzed by immunoblotting with anti-phosphoamino acid antibody (top) and anti-GFP antibody (bottom). Where noted (right panel), anti-GFP Immunoprecipitates were treated with lambda phosphatase for 2 h. All data represent a minimum of 3 biological replicates. **(B)** SILAC analysis of relative phosphorylation levels at position S196 and T199 of Mdh1-GFP on day 2 of incubation in SL medium. Samples were collected from *AUP1* (strain PKY520, heavy) and *aup1Δ* (strain PKY661, light) cells as described in "Methods", and anti-GFP immunoprecipitates were analyzed by LC-MS/MS to determine the ratio of phosphopeptides in WT versus *aup1Δ* cells.

Figure 7. Expression of the 'hypermitophagic' *MDH1* mutant T199D can suppress the *aup1Δ* and *pkp2Δ* phenotypes, and Pkp2 functions downstream of Aup1. *C*ells (PKY365) expressing WT Mdh1-GFP, as well as **(A)** *aup1Δ* (PKY456) or **(B)** *pkp2Δ* (PKY488) cells expressing WT Mdh1-GFP and the indicated Mdh1 variants (all constructs were expressed from the endogenous *MDH1* promoter) were incubated in SL medium for 5 days and protein extracts were prepared. Equal amounts of protein (20 µg) were subjected to SDS-PAGE and immunoblotting with anti-GFP antibody. The % free GFP was normalized relative to WT Mdh1-GFP, for each variant. **(C) Overexpression of Pkp2, but not Pkp1, can bypass the *aup1Δ* block in Mdh1 mitophagic trafficking**. Pkp1 and Pkp2 were overexpressed from the *CUP1* promoter. (D) **Overexpression of Pkp2 leads to recovery of Mdh1-GFP phosphorylation in the *aup1Δ* background**. TVY1 (control) and PKY395 (*aup1Δ*) cells, expressing Pkp2 or harboring empty vector (*φ*) were grown in SL medium for the indicated times and Mdh1-GFP was immunoprecipitated under native conditions and analyzed by immunoblotting with anti pSer/pThr antibodies. Data are representative of at least 3 biological replicates.

Figure 8. Loss of Aup1 affects protein-protein interactions of Mdh1. Wild-type and *aup1Δ* cells (PKY826, PKY827, PKY824, PKY825) expressing either Mic60-HA or Cit1-HA from the respective endogenous promoters were grown for 1 or 4 days in synthetic lactate medium, and native extracts (prepared as detailed in "Materials and Methods") were immunoprecipitated with anti-GFP antibodies. The immunoprecipitates were analyzed by immunoblotting with anti-HA antibodies. **(A)** loss of Aup1 affects the interaction between Mdh1 and Mic60. **(B)** loss of Aup1 affects the interaction between Mdh1 and Cit1. Data are representative of at least 3 independent biological replicates.

Figure 9. Phosphorylation state affects the matrix distribution of Mdh1-GFP.

A. **Deletion of *AUP1* affects distribution of Mdh1-GFP within the mitochondrial matrix.** Cells (*mdh1Δ*) co-expressing Mdh1-GFP from the endogenous promoter and a generic mtRFP were imaged on days 1 and 2 of the incubation (to avoid interference from vacuolar signal, top panels) and the overlap between the red and green channels was quantified as described in 'Materials and Methods'. Graph (bottom) shows quantification of the overlap between the two channels and statistical significance (NS, not significant). **B**. **The T199A and S196A mutations also increase the**

segregation of Mdh1-GFP, relative to a matrix mtRFP. Cells (*mdh1Δ*) expressing the indicated Mdh1-GFP species and a generic mtRFP were imaged and analyzed as in **A**. Results are representative of two biological replicates. Scale bar =1 μm.

Figure 10. A model for the role of protein phosphorylation in regulating mitophagic selectivity. We suggest that phosphorylation of mitochondrial matrix proteins such as Mdh1 can regulate their tendency to undergo mitophagy, within the matrix. (1) Increased phosphorylation of T199 and decreased phosphorylation at S240 bring about a change in protein-protein interactions that leads to segregation of this species. (2) multiple fusion and fission events lead to a 'distillation' like process that enriches this species in a single mitochondrial compartment, along with other protein species with similar properties. (3) A final fission event generates a mitochondrion sufficiently enriched in 'degradation-bound' species. We hypothesize that the proteostatic load in this compartment generates a signal which activates the Atg32 receptor, possibly through Yme2-dependent clipping of the Atg32 C-terminus, leading to engulfment of this compartment- with its enclosed protein components- by autophagic sequestering membranes.

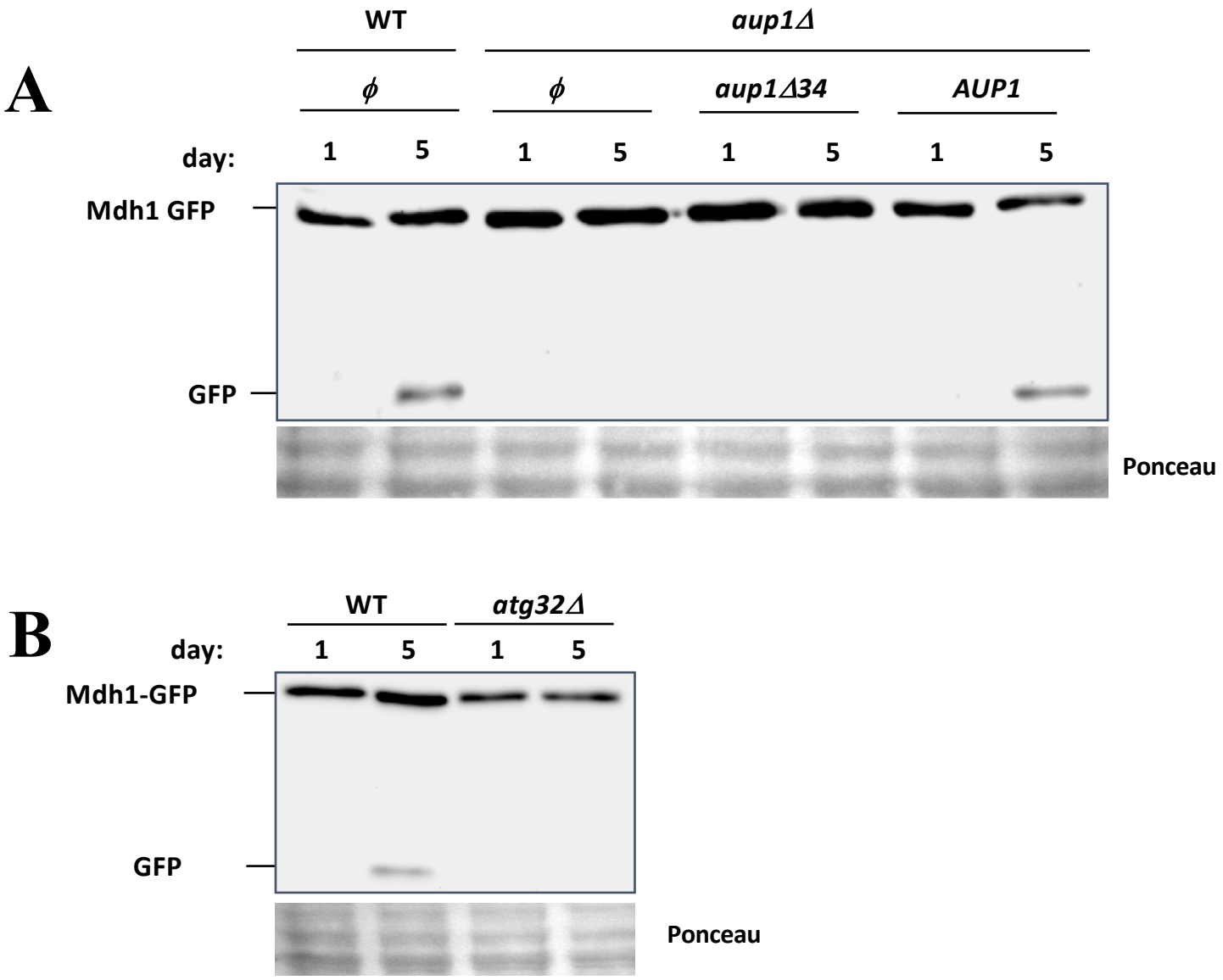
A
WT
aup1Δ
ϕ
ϕ
aup1Δ34
AUP1
day:
1
5
1
5
1
5
1
5
Mdh1 GFP
GFP
Ponceau
B
WT
atg32Δ
day:
1
5
1
5
Mdh1-GFP
GFP
Ponceau

Figure 1

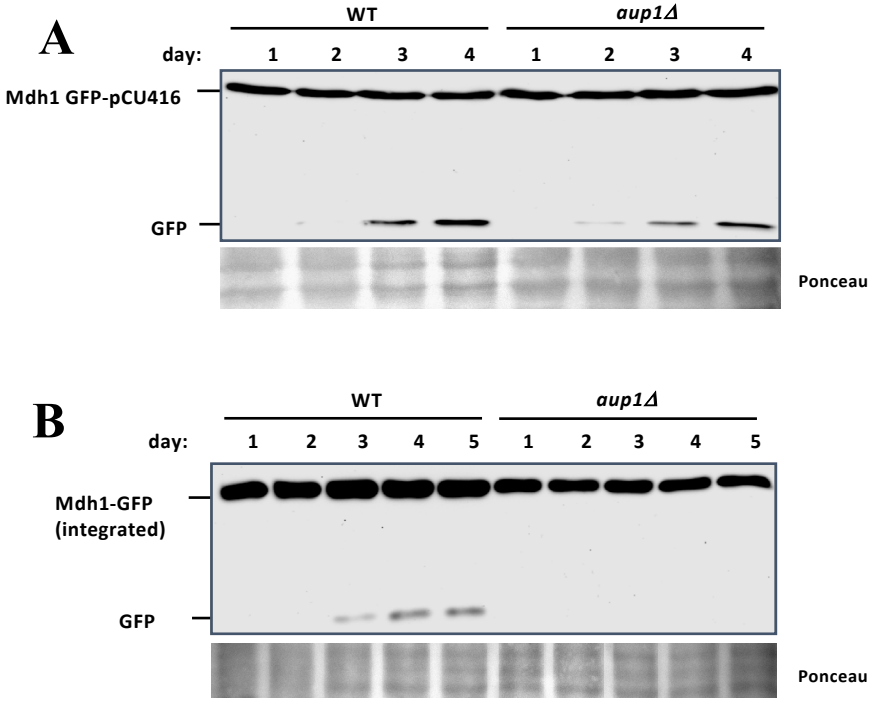
A
WT
aup1Δ
day:
1 2 3 4 1 2 3 4
Mdh1 GFP-pCU416
GFP
Ponceau
B
WT
aup1Δ
day:
1 2 3 4 5 1 2 3 4 5
Mdh1-GFP
(integrated)
GFP
Ponceau
C
WT
aup1Δ
day:
1 2 3 4 1 2 3 4
Idp1-GFP-pCU416
GFP
Ponceau
D
WT
aup1Δ
day:
1 2 3 4 5 1 2 3 4 5
Idp1-GFP
(integrated)
GFP
Ponceau

Figure 2

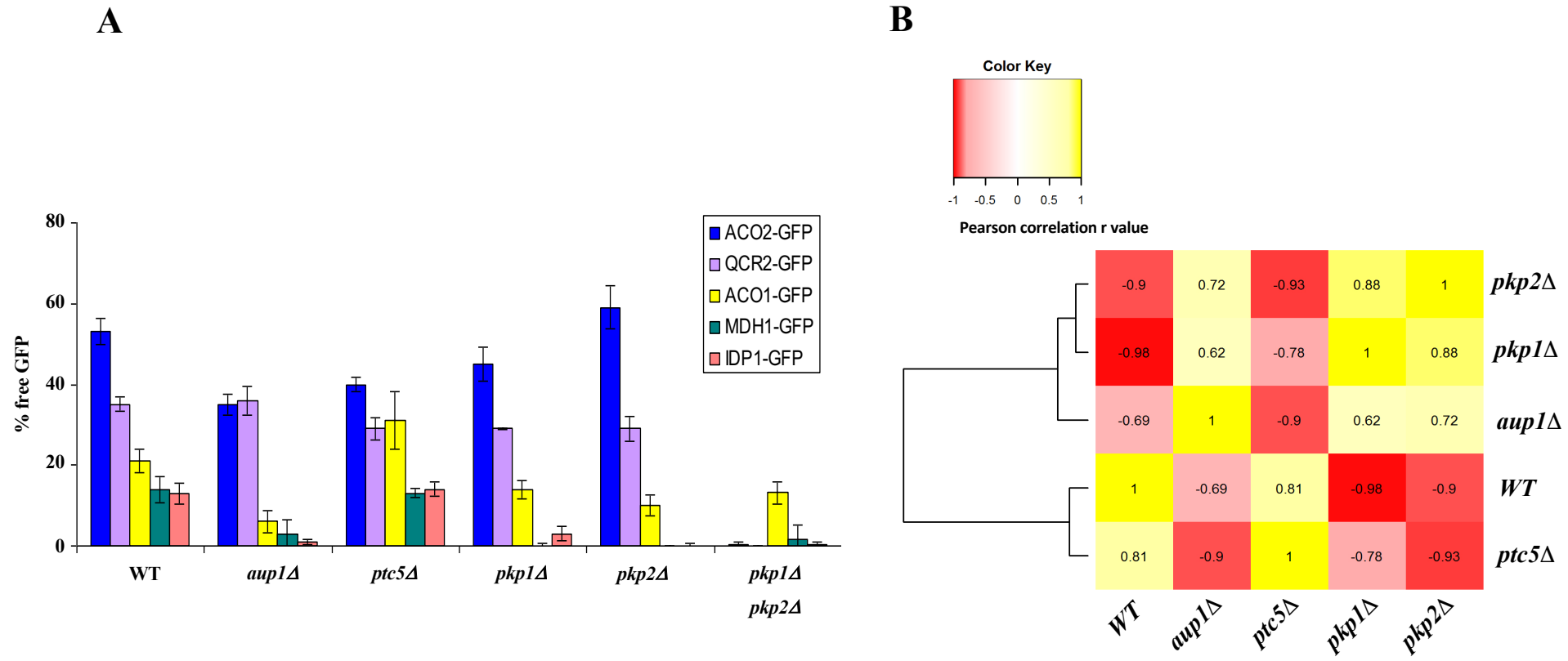
A
B
% free GFP
80
60
40
20
0
ACO2-GFP
QCR2-GFP
ACO1-GFP
MDH1-GFP
IDP1-GFP
WT
aup1Δ
ptc5Δ
pkp1Δ
pkp2Δ
pkp1Δ pkp2Δ
Color Key
-1 -0.5 0 0.5 1
Pearson correlation r value
-0.9 0.72 -0.93 0.88 1
-0.98 0.62 -0.78 1 0.88
-0.69 1 -0.9 0.62 0.72
1 -0.69 0.81 -0.98 -0.9
0.81 -0.9 1 -0.78 -0.93
pkp2Δ
pkp1Δ
aup1Δ
WT
ptc5Δ
WT
aup1Δ
ptc5Δ
pkp1Δ
pkp2Δ

Figure 3

A

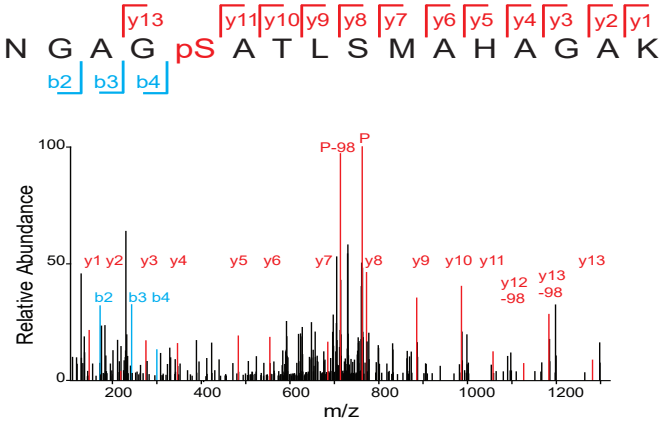
y13 y11 y10 y9 y8 y7 y6 y5 y4 y3 y2 y1
N G A G pS A T L S M A H A G A K
b2 b3 b4
P-98 P
y1 y2 y3 y4 y5 y6 y7 y8 y9 y10 y11 y12 -98 y13 -98 y13
b2 b3 b4
Relative Abundance
m/z

B

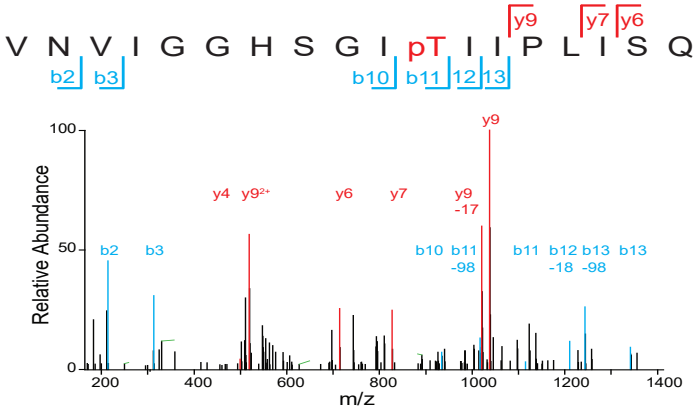
y9 y7 y6 y4
V N V I G G H S G I pT I I P L I S Q T N H K
b2 b3 b10 b11 12 13
y9
y4 y9²⁺ y6 y7 y9 -17
b2 b3 b10 b11 -98 b11 b12 -18 b13 -98 b13
Relative Abundance
m/z

C

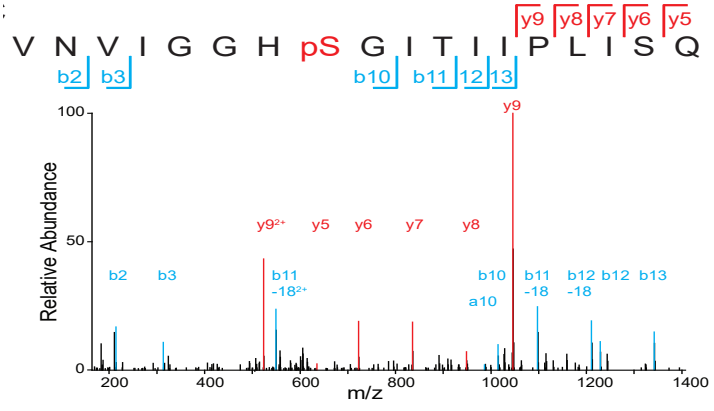
y9 y8 y7 y6 y5
V N V I G G H pS G I T I I P L I S Q T N H K*
b2 b3 b10 b11 12 13
y9
y9²⁺ y5 y6 y7 y8
b2 b3 b11 -18²⁺ b10 a10 b11 -18 b12 b12 -18 b13
Relative Abundance
m/z

Figure 4

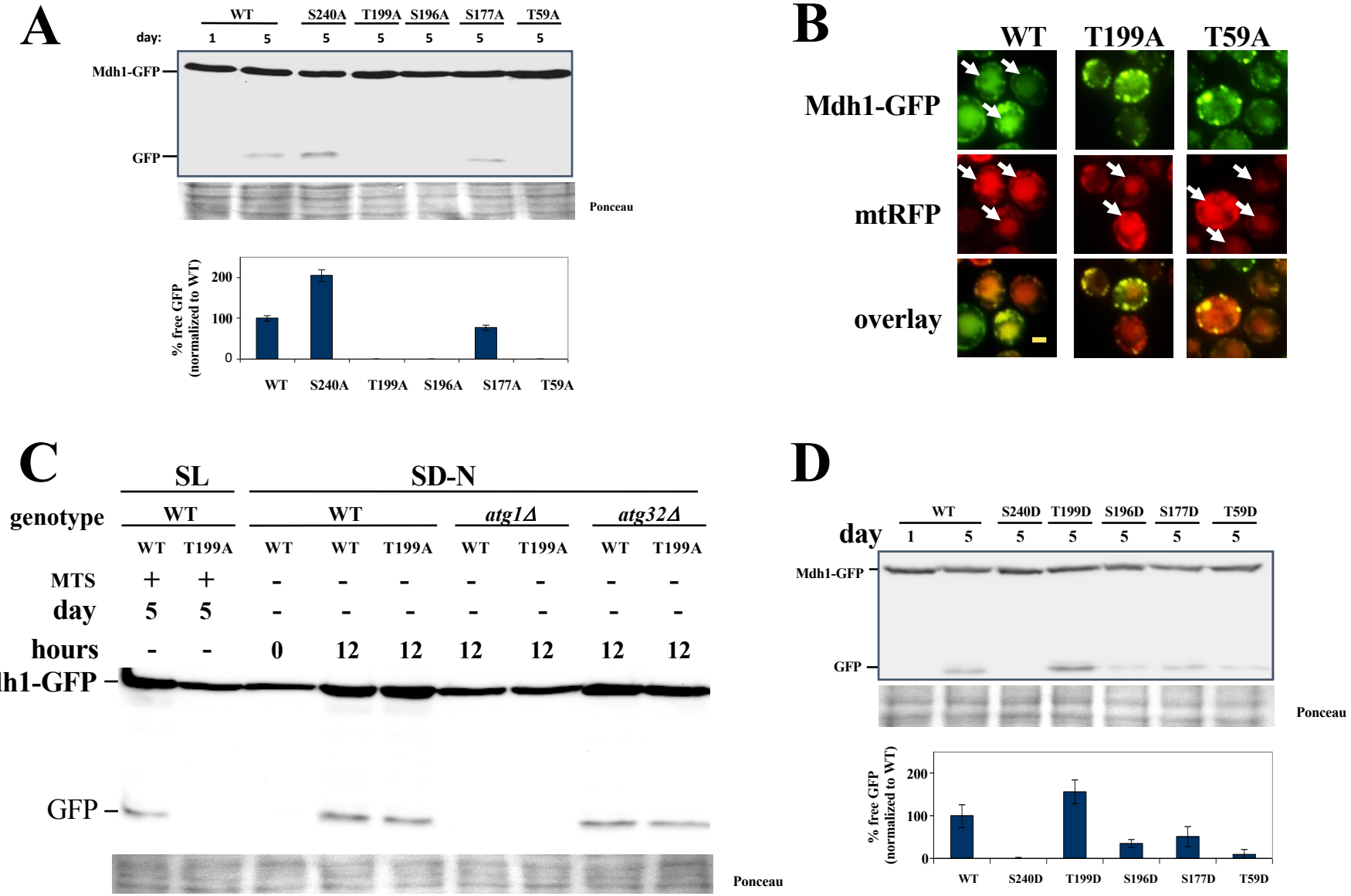
A
WT
S240A
T199A
S196A
S177A
T59A
day:
1
5
5
5
5
5
5
Mdh1-GFP
GFP
Ponceau
% free GFP (normalized to WT)
200
100
0
WT
S240A
T199A
S196A
S177A
T59A
B
WT
T199A
T59A
Mdh1-GFP
mtRFP
overlay
C
SL
SD-N
genotype
WT
WT
atg1Δ
atg32Δ
WT
T199A
WT
WT
T199A
WT
T199A
WT
T199A
MTS
+
+
-
-
-
-
-
-
-
day
5
5
-
-
-
-
-
-
-
hours
-
-
0
12
12
12
12
12
12
Mdh1-GFP
GFP
Ponceau
D
day
WT
S240D
T199D
S196D
S177D
T59D
1
5
5
5
5
5
5
Mdh1-GFP
GFP
Ponceau
% free GFP (normalized to WT)
200
100
0
WT
S240D
T199D
S196D
S177D
T59D

Figure 5

A

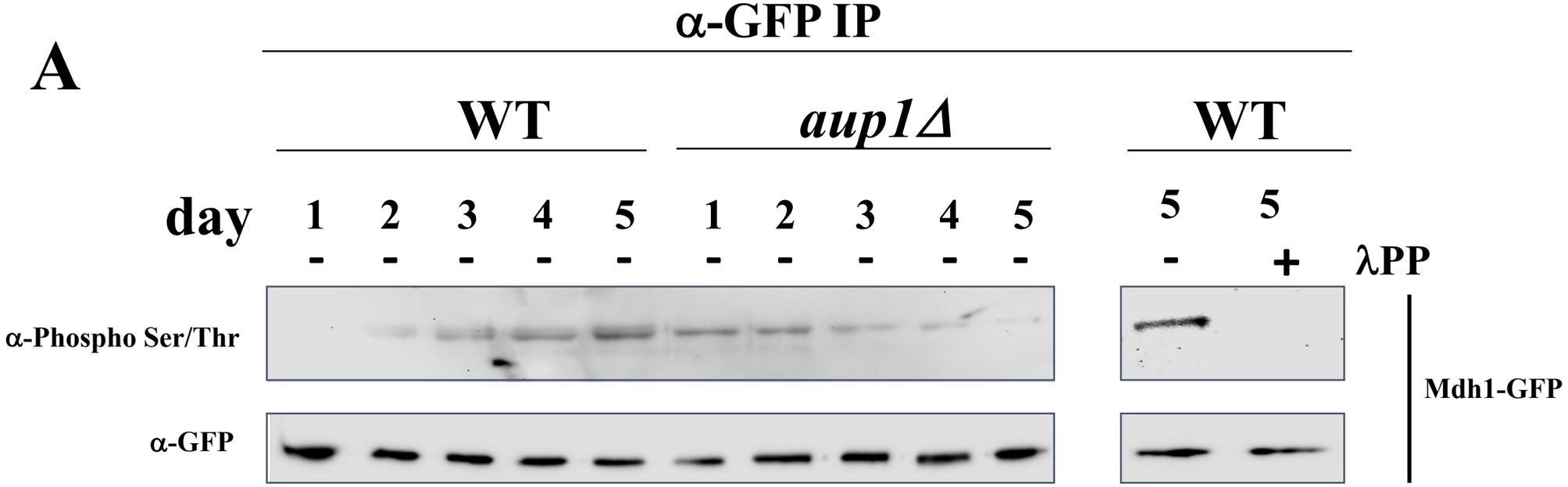
α-GFP IP
WT
aup1Δ
WT
day
1 2 3 4 5 1 2 3 4 5
5 5
- - - - - - - - - - - +
λPP
α-Phospho Ser/Thr
α-GFP
Mdh1-GFP

B

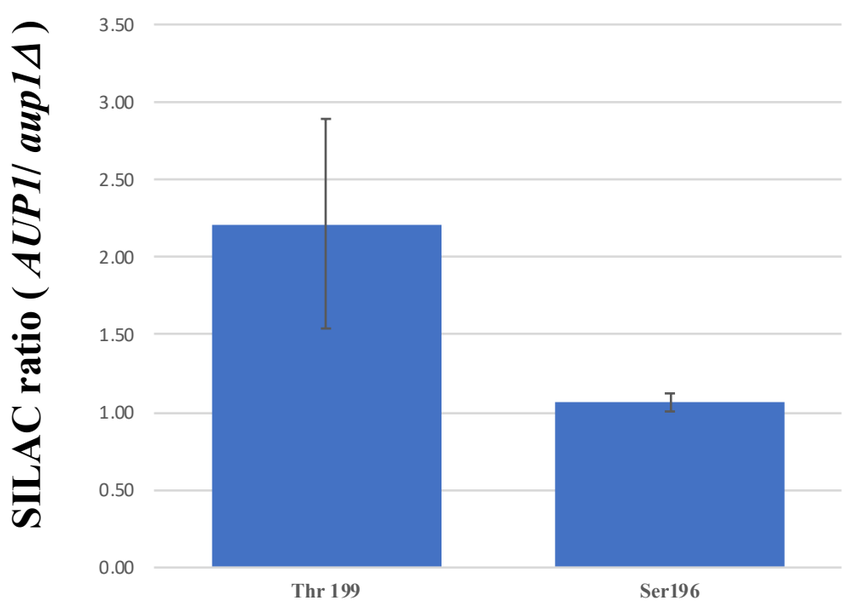
SILAC ratio (AUP1/ aup1Δ)
3.50
3.00
2.50
2.00
1.50
1.00
0.50
0.00
Thr 199
Ser196

Figure 6

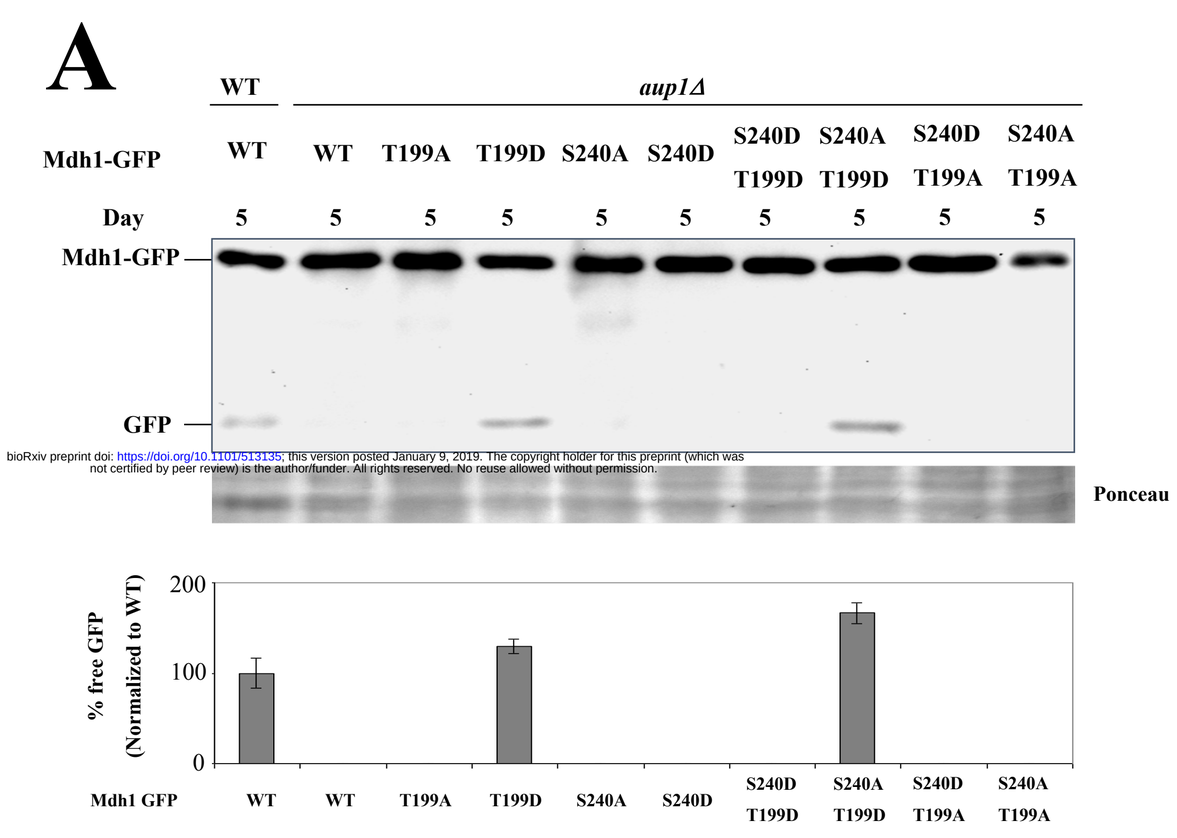

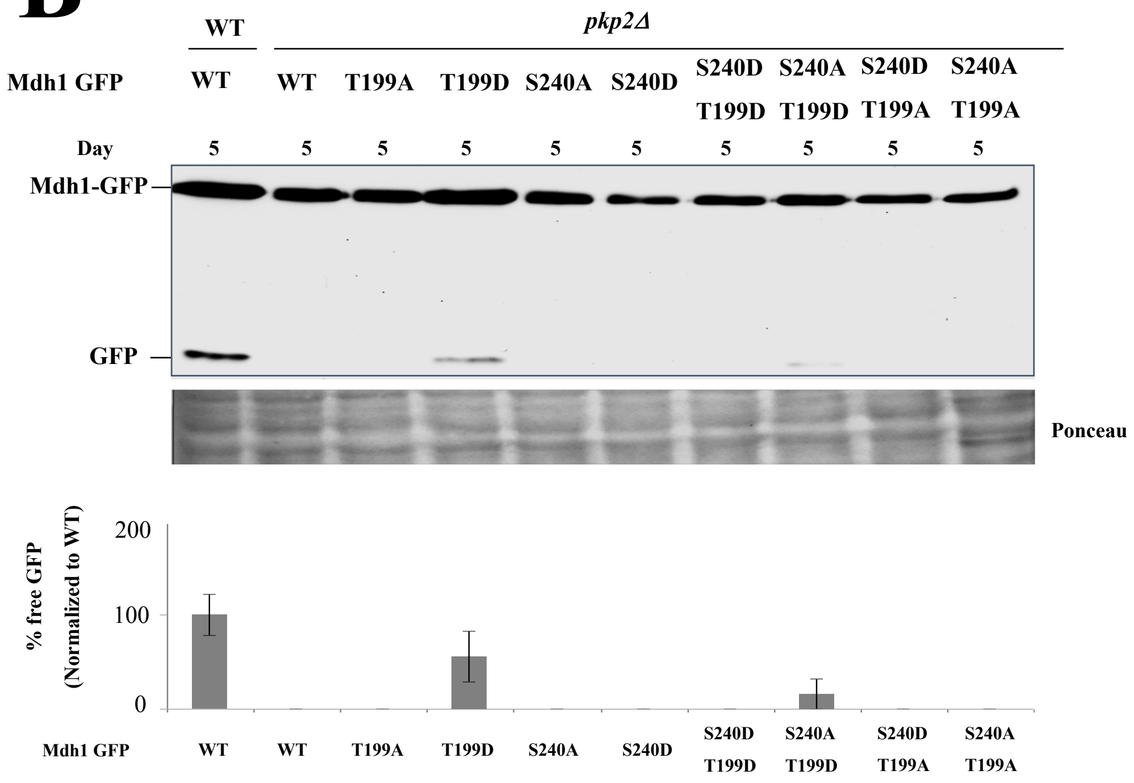

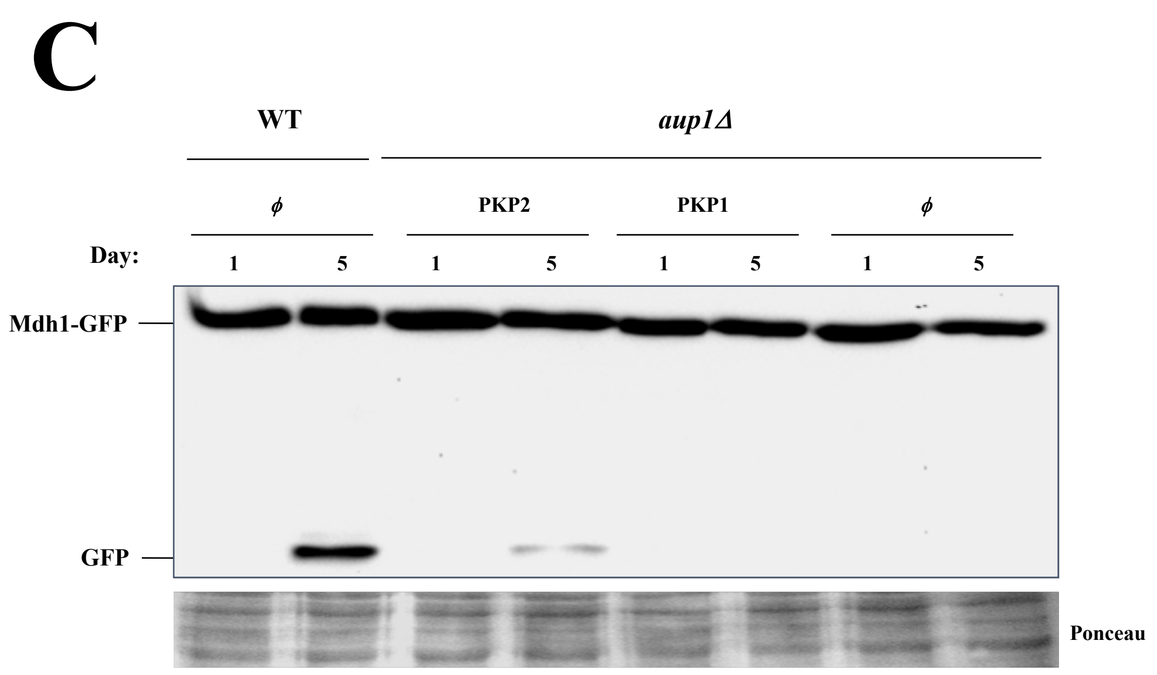

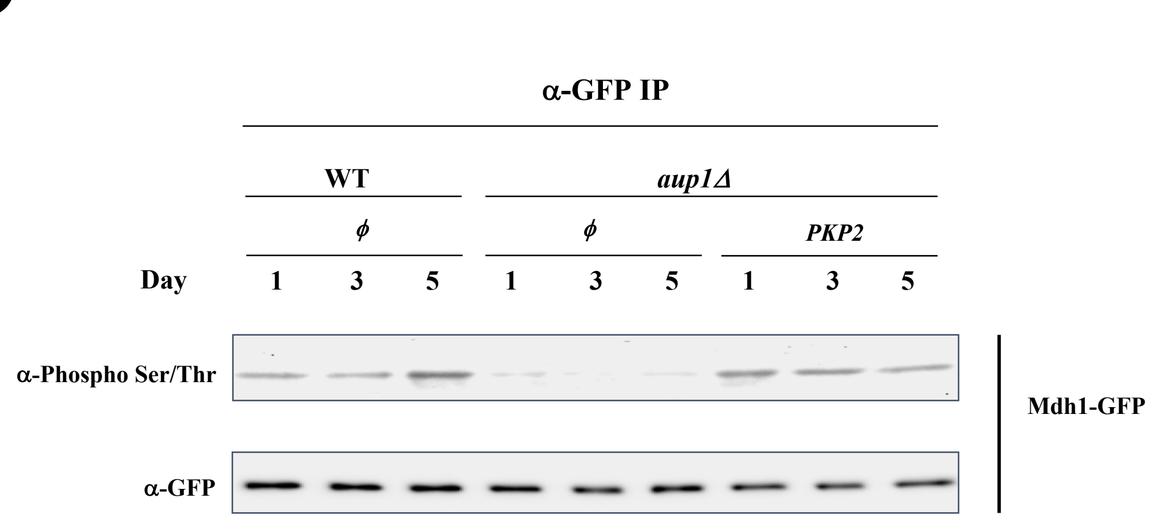

Figure 7

A

α-GFP IP

	WT	WT	WT	*aup1Δ*	WT	*aup1Δ*
Mic60-HA	+	-	+	+	+	+
Mdh1-GFP	-	+	+	+	+	+
Day	1	1	1	1	4	4

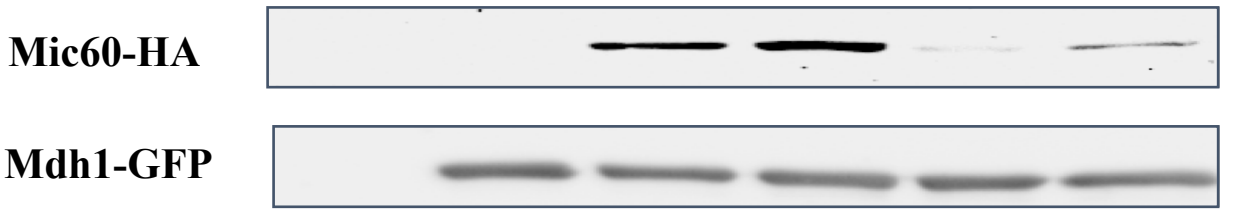

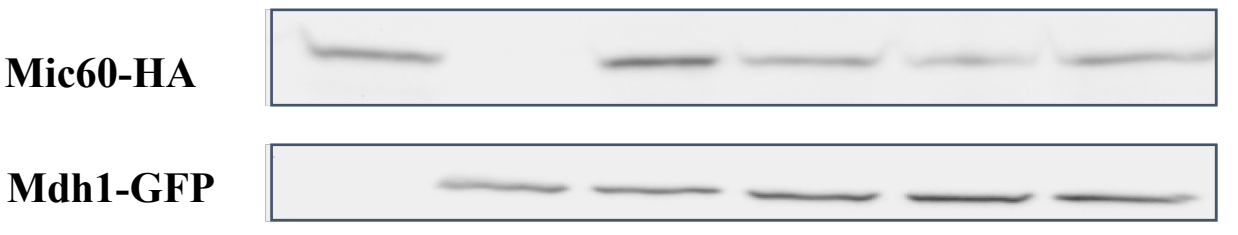

Input (3% of total)

B

α-GFP IP

	WT	WT	WT	*aup1Δ*	WT	*aup1Δ*
Cit1-HA	+	-	+	+	+	+
Mdh1-GFP	-	+	+	+	+	+
Day	1	1	1	1	4	4

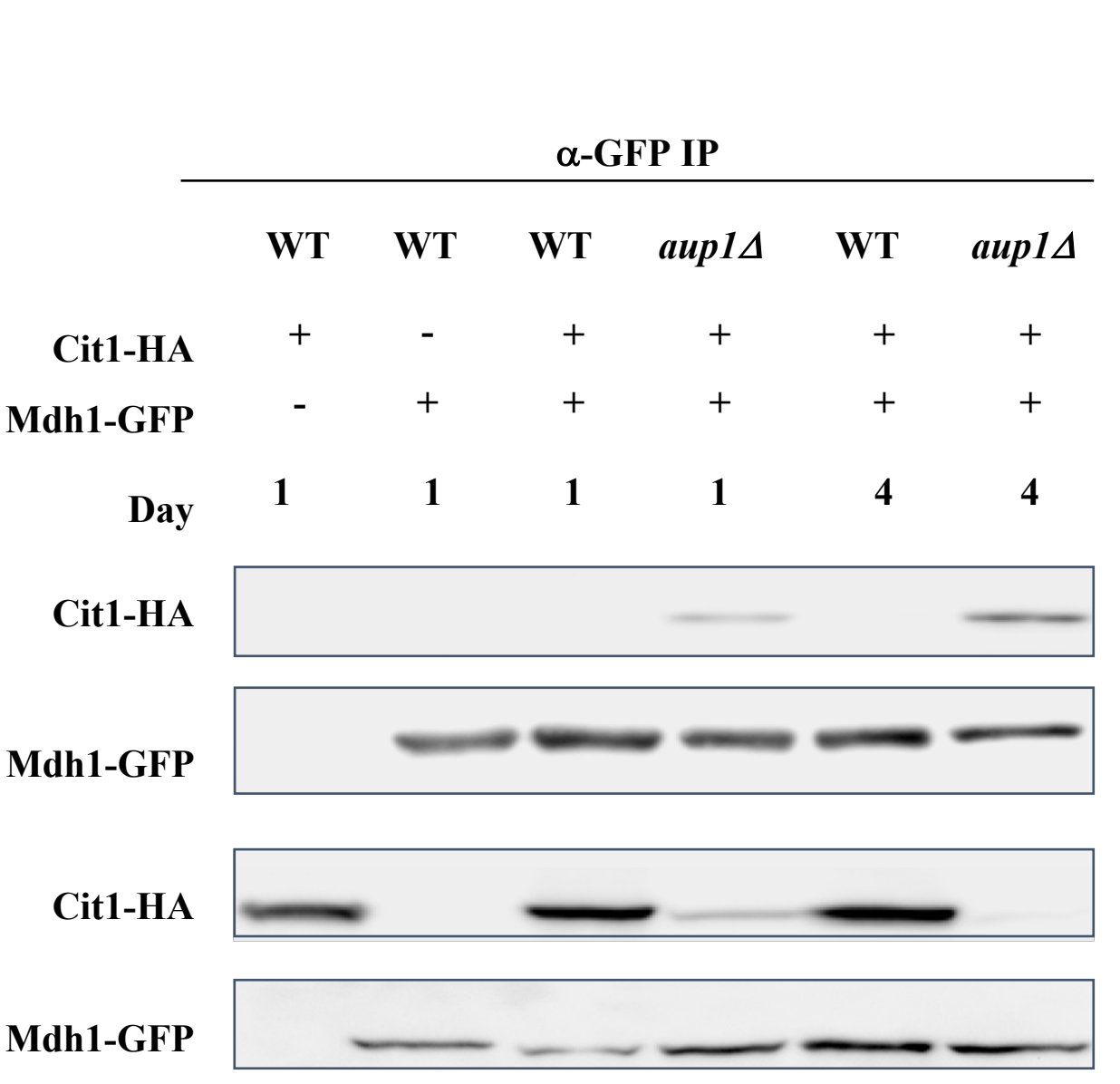

Input (3% of total)

Figure 8

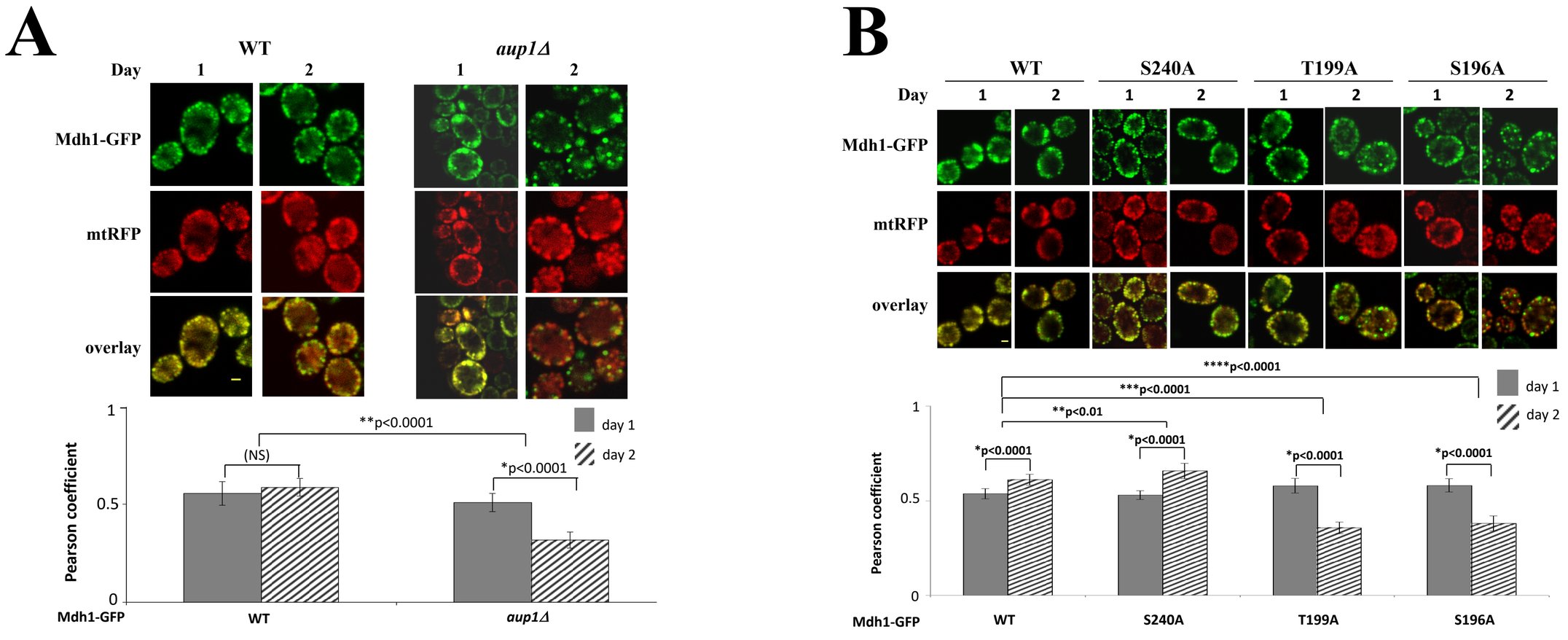
A
WT
aup1Δ
Day
1
2
1
2
Mdh1-GFP
mtRFP
overlay
Pearson coefficient
1
0.5
0
**p<0.0001
(NS)
*p<0.0001
day 1
day 2
Mdh1-GFP
WT
aup1Δ
B
WT
S240A
T199A
S196A
Day
1
2
1
2
1
2
1
2
Mdh1-GFP
mtRFP
overlay
****p<0.0001
***p<0.0001
**p<0.01
*p<0.0001
*p<0.0001
*p<0.0001
*p<0.0001
day 1
day 2
Pearson coefficient
1
0.5
0
Mdh1-GFP
WT
S240A
T199A
S196A

Figure 9

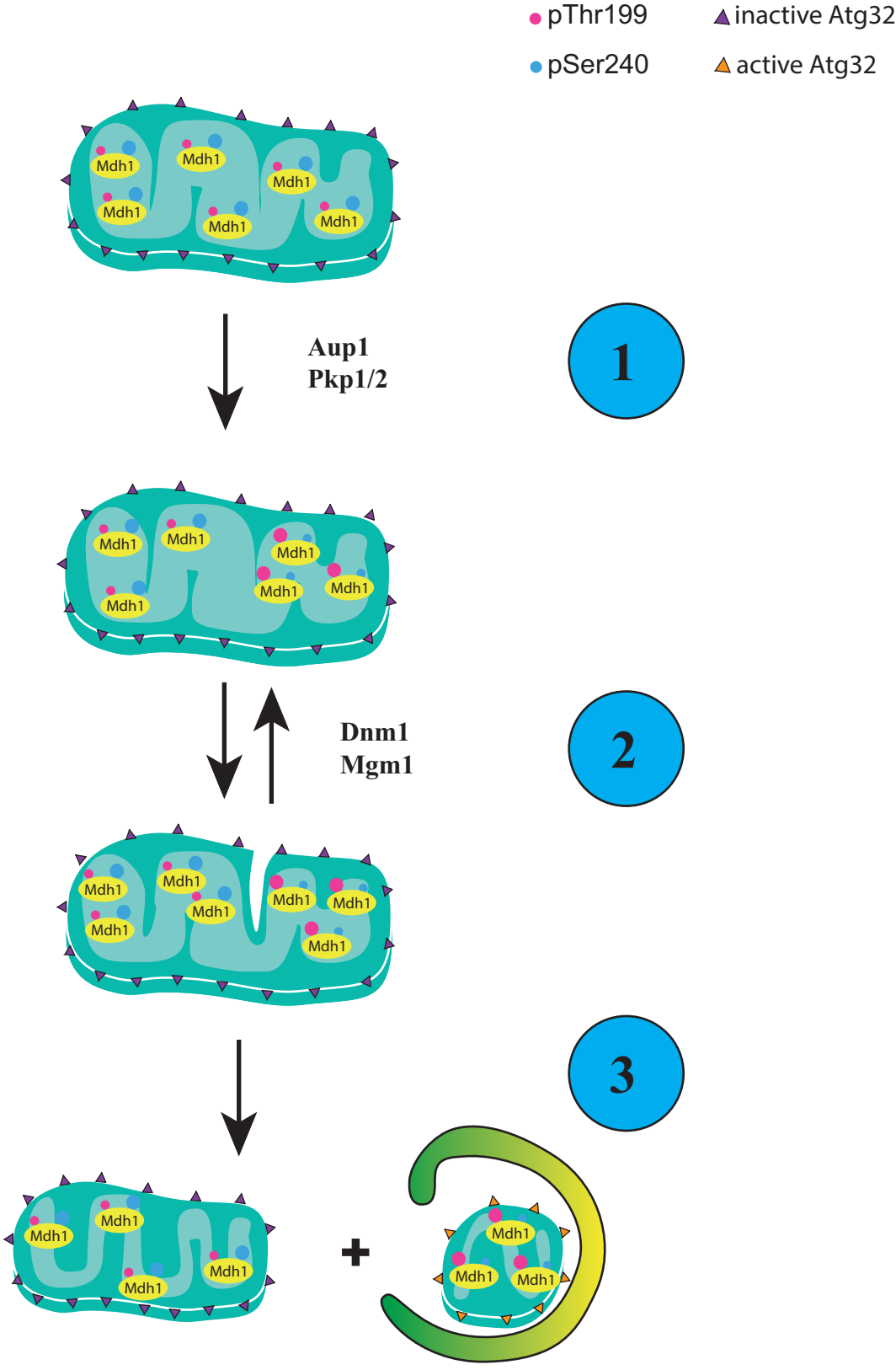
pThr199
pSer240
inactive Atg32
active Atg32
Mdh1
Aup1
Pkp1/2
1
Dnm1
Mgm1
2
3

Figure 10